Proceedings of the 5th U.S.-Japan Natural Resources Meeting and Parkfield, California Fieldtrip

By Shane T. Detweiler[1] and William Ellsworth[1]

Open-File Report 2005-1131

2005

U.S. DEPARTMENT OF THE INTERIOR
U.S. GEOLOGICAL SURVEY

[1]Menlo Park, Calif.

The 2003 M6.5 San Simeon and 2004 M6.0 Parkfield earthquakes in central California.

Jeanne Hardebeck, U.S. Geological Survey, Menlo Park, CA, jhardebeck@usgs.gov

The M_W6.5 San Simeon earthquake struck the central California coast on December 22, 2003. The earthquake occurred on a NW–striking reverse fault dipping to the NE. Although motion along the Pacific-North American plate boundary in California is dominantly strike-slip, there is a small compressional component through central California, uplifting the Coast Ranges. No surface rupture associated with the earthquake has been identified.

The San Simeon rupture was fairly simple, with the majority of slip taking place in a single slip patch SE of the hypocenter. The earthquake ruptured unilaterally to the SE, and the effects of directivity are apparent in the strong ground motion records. The strong SE directivity resulted in a concentration of damage to the SE of the hypocenter. The worst earthquake damage occurred in Paso Robles, 40 km to the SE of the epicenter, primarily to unreinforced brick buildings. Brick buildings that had been seismically retrofit, in general, performed much better than those that had not been retrofit.

Aftershocks have concentrated in two areas: one near the mainshock hypocenter, and the other to the SE. The low-seismicity gap between the two major clusters corresponds to the peak slip of the mainshock. The aftershocks in the region of the mainshock hypocenter delineate the NE-dipping mainshock plane and a SW-dipping conjugate plane. The cluster to the SE is more diffuse. A mixture of thrust and strike-slip focal mechanisms is observed, both with compression axes trending NE. The rate of aftershocks following San Simeon is slightly higher than average for California, and the decay rate is slightly slower than average.

The M_W6.0 Parkfield earthquake occurred approximately 50 km away and 9 months later, on September 28, 2004. The mainshock occurred on the San Andreas Fault, a right-lateral strike-slip fault that accommodates the majority of Pacific-North American plate motion. The mainshock ruptured unilaterally to the NW, and the majority of aftershocks occurred to the NW of the mainshock epicenter along the San Andreas. The aftershock rate following the Parkfield earthquake is typical of California.

The proximity of the San Simeon and Parkfield earthquakes to each other in space and time suggests that the San Simeon sequence may have triggered the Parkfield event. Static stress change modeling shows that the San Simeon mainshock increased the Coulomb stress on the San Andreas near Parkfield by 0.03-0.1 bar, primarily due to a decrease in normal stress.

The Parkfield earthquake occurred on the same part of the fault that ruptured previously in similar-sized events in 1857, 1881, 1901, 1922, 1934, and 1966. Because of the regular nature of earthquakes on this fault segment, an event at Parkfield was anticipated and this part of the fault was highly instrumented. The Parkfield earthquake is therefore one of the best-recorded earthquakes in the world.

The southeastern Kii Peninsula earthquake (M7.4) of September 5, 2004, A Quick Report

Yoshimitsu Okada, Coordinating Committee for Earthquake Prediction (CCEP), Japan,
okada@bosai.go.jp

Introduction

An earthquake of M7.4 occurred southeast of the Kii Peninsula, central Japan, on 23h57m(JST) of Sep. 5, 2004. The epicenter was located near the Nankai trough axis close to the focal region of the 1944 Tonankai earthquake (M7.9). The focal mechanism showed a reverse fault solution with NS-compression, and the focal depth was estimated to be around 20 km suggesting an intra-plate event. A weak tsunami was also recorded (max. height of 0.9 m) and a southward co-seismic crustal deformation (max. 5.2 cm) was detected by GPS observations.

Earthquake sequence

About 5 hours before to the main shock, there was a foreshock of M6.9 40 km away to the WSW. Aftershocks were aligned in two directions, i.e. along the Nankai trough, and almost perpendicular to the trough. In the aftershock sequence, two M6 class events occurred (M6.4 on 9/7 08h29m and M6.5 on 9/8 23h58m).

The ocean bottom topography has linear structures that cross the trough which may correspond to the NW-SE trending aftershock distribution.

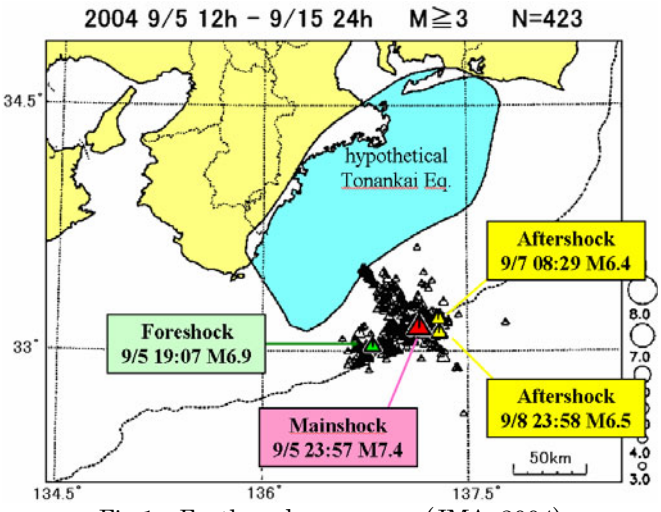

Fig.1 Earthquake sequence (JMA, 2004)

Historical record

Along the Nankai trough, the seismicity is generally low. Dr. Ohtake, the President of CCEP, investigated the seismic activity before the 1944 Tonankai and 1946 Nankai earthquakes. During the 80 years from 1885-1943, he found a sequence of moderate earthquakes of M6 or larger along the trough. They were 1917 (M6.0), 1919 (M6.0), 1922 (M6.1), 1923 (M6.3) and 1938 (M6.8). The epicenter of the earthquake of Sep. 5, 2004 was quite near to that of the 1917 event.

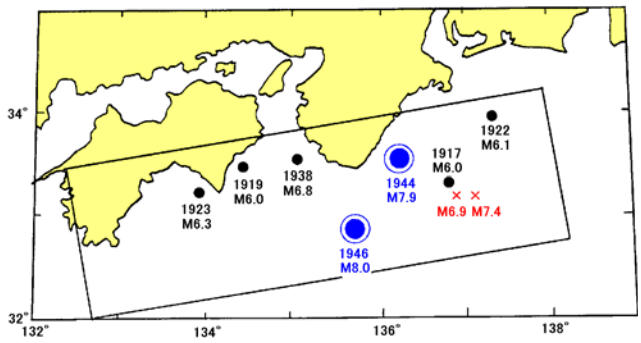

Fig.2 Earthquakes of M≧6 and H<100km in 1885-1943 (Ohtake,2004)

Focal mechanism

All the focal mechanisms of the foreshock, main shock, and two M6 class aftershocks

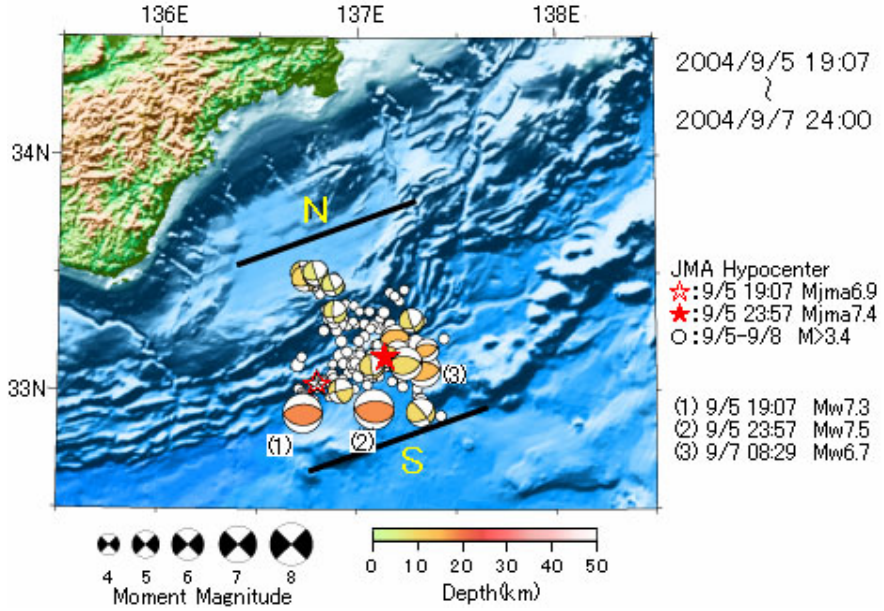

Fig. 3. Spatial distribution of CMT (NIED, 2004)

show reverse fault solutions with a NS compression axis. However strike-slip events can be seen in the northern part of the aftershock branch perpendicular to the Nankai trough.

In general, normal faulting events are dominant along the trough axis. However, in the region surrounding the main shock, it was found that similar reverse fault events have also been generated in the past. The results of multiple seismic reflection surveys in this area indicate the existence of north-dipping reverse faults within the Philippine Sea plate as well as a strike-slip structure crossing the trough.

Focal depth and aftershock distribution

Since this event has occurred offshore, we cannot expect good focal depths. Although we tried to redetermine hypocenters, the ambiguity of the crustal structure strongly affects the results and we cannot get a definite answer at present.

Crustal deformation and tsunami

Associated with the main shock, clear coseismic deformation was detected in a wide area of central Honshu by GPS observation. At the Shima station, in the eastern Kii Peninsula, a southward displacement of 5.2 cm was detected. Also, the main shock and foreshock generated weak tsunamis. At Kushimoto station, in the southern tip of the Kii Peninsula, a height of 0.9 m was recorded for main shock and 0.3 m for foreshock.

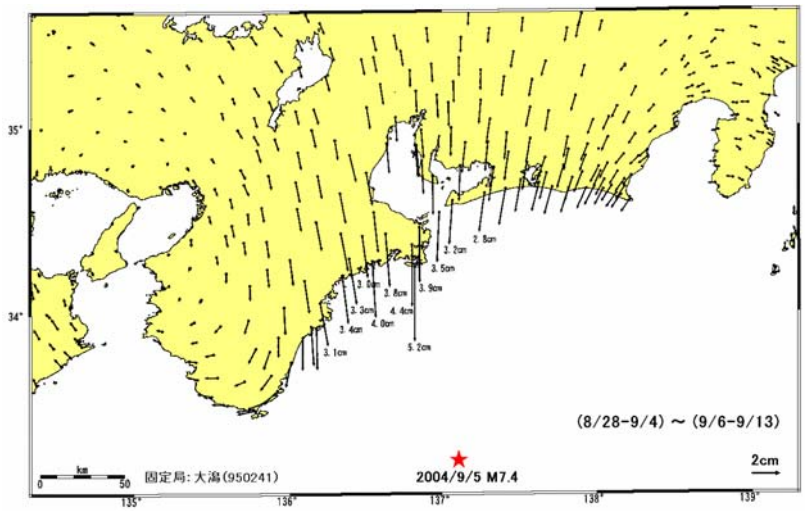

Fig.4 Horizontal displacement detected by GPS (GSI,2004)

Fault model

Several fault models are proposed for this event. The Geographical Survey Institute

proposed a simple model of WSW-ENE strike and north dipping faults to explain the GPS data. Dr. Yamanaka of the Earthquake Research Institute analyzed broadband waveforms from IRIS-DMC and concluded that the main shock was generated by a NW-SE strike and southward dipping fault. On the other hand, Dr. Yagi of Building Research Institute proposed a multi-fault model composed of an EW striking, southward-dipping fault and NW-SE striking vertical strike-slip fault to get a better fit to the waveforms.

Ocean bottom observation

As was seen in the preceding section, the image of this earthquake is somewhat ambiguous. Some confusion remains regarding focal mechanism, aftershock distribution and the fault model. We are expecting key data from ocean bottom observation. The University group set up an array of pop-up type ocean bottom seismometers around the focal region, some of which were already retrieved, and the analysis is ongoing. The Hydrographic and Oceanographic Department of the Japan Coast Guard is resurveying the position of ocean bottom benchmarks combining GPS and acoustic ranging. We hope these key data will help to constrain the model parameters.

Triggered ultra-low frequency events around Nankai trough

It is known that ultra-low frequency events are occasionally generated at very shallow zones near the Nankai trough. Four months prior to the occurrence of this M7.4 earthquake, concentrated activity of ultra-low frequency events occurred just south of the Kii Peninsula. After the M7.4 earthquake, more extensive ultra-low frequency events occurred in the focal region as well as at Kii Channel, to the SW off the Kii Peninsula. These events seem to be triggered by seismic activity including the M7.4 earthquake.

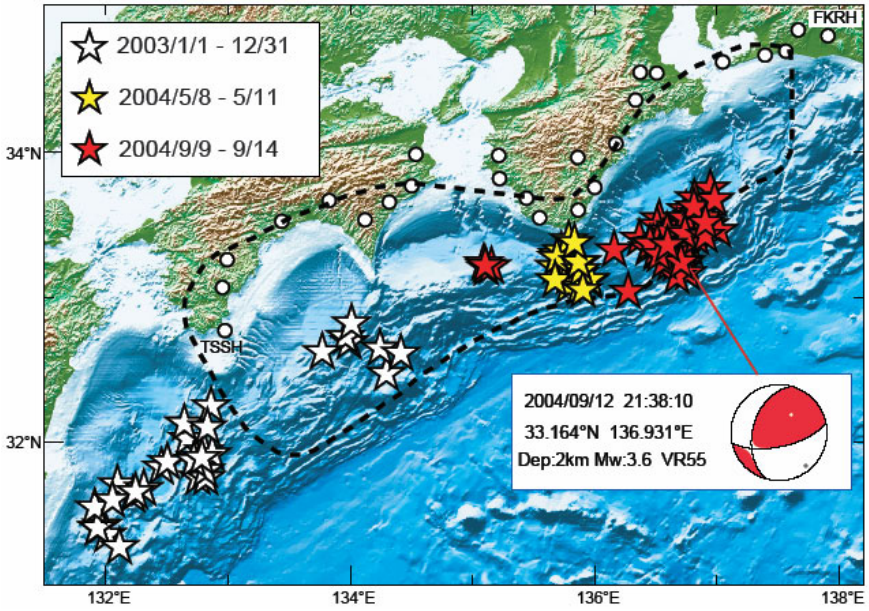

Fig.5 Ultra low-frequency events along Nankai trough (Obara,2004)

Rapid Post-Earthquake Information Tools from the Advanced National Seismic System (ANSS)

David J. Wald, U. S. Geological Survey, Golden, CO, wald@usgs.gov

To better serve the United States emergency management and response, engineering, and scientific communities, more and better seismic data are being collected and more powerful and useful data products are being developed under the auspices of the Advanced National Seismic System (ANSS) by the U.S. Geological Survey and its ANSS partners in academia, government, and industry. New, rapid analyses are available via our web sites for which distributed servers provide both bandwidth and redundancy during earthquake disasters. ***Recent Earthquake Maps***, ***Earthquake in the News***, and ***Earthquake Summary Posters*** provide rapid, post-earthquake summaries of seismicity, tectonic context, earthquake effects, and other important information for significant events, not only nationally, but also globally. In addition, we are moving beyond enhanced earthquake web pages to push earthquake information to users who have a need for near real-time earthquake analysis. One such notification product is ***CISN Display***, an application for visualization of seismicity and ground shaking for critical users developed primarily by the ANSS California Integrated Seismic Network (CISN) partners. The first release of **QWEmailer**, also now available from CISN, enables users to automatically issue earthquake notification (email and short text messages) specific to their needs. The ANSS is complementing CISN advances through ongoing development of ***ShakeMap***, a tool used to portray the extent of potentially damaging ground shaking following an earthquake, and with ***ShakeCast*** (http://www.shakecast.org/), an application for automating ShakeMap delivery to users and facilitating notification of shaking levels at user-selected facilities. Finally, we describe advancing uses of and development of ***"Did You Feel It?"***, a popular citizen-science, internet-based tool for rapidly mapping post-earthquake seismic intensities, which is particularly useful in areas of the U.S. not yet well covered by ANSS instrumentation. The development of these and other products will be discussed in detail. These applications are changing and improving rapidly; up-to-date earthquake information is available online at http://earthquake.usgs.gov/ and links to new software can be found at http://www.cisn.org/software/. These products rely fundamentally on magnitudes, hypocenters, and ground motion data, including urban arrays, collected and interpreted at regional and national seismic data centers under the ANSS. Improvement in accuracy and quality of these critical products depends directly on the growing national investment on more instruments in urban settings.

The challenge of earthquake disaster mitigation
- Earthquake Early Warning and Estimated Seismic Intensity -

Shin'ya Tsukada, Japan Meteorological Agency, tsukada@met.kishou.go.jp

Several efforts to mitigate disasters caused by earthquakes and volcanic activity have been made by one of the most important national programs in Japan. The Japan Meteorological Agency (JMA) is the governmental organization that is responsible for tsunami forecasts, earthquake prediction of the Tokai earthquake, and release of information on various other earthquakes, tsunamis and volcanic activity.

JMA developed the seismic intensity meter in 1991 to enable objective seismic intensity measurement with higher spatial resolution and faster collection of data than had been available using human judgment and site inspection. JMA disseminates quick seismic intensity reports within about two minutes after an earthquake, and the report is utilized to set-up emergency countermeasures by relevant disaster mitigation organizations. However, there remain two problems; the report is still post-disaster information, and there is no way to infer the seismic intensity at a place where no seismic intensity meter is installed.

JMA is now developing two new technologies to solve these problems by utilizing up-to-date computer performance, a high speed communications link, and our latest knowledge on seismic wave propagation. These projects are known as 'Earthquake Early Warning' and 'Estimated Seismic Intensity'.

'Earthquake Early Warning' enables countermeasures to begin before the strong motion arrival by estimating the hypocenter and magnitude using seismic waveform data observed at the stations close to the epicenter, and by issuing estimated seismic intensity before the strong motion arrival. We adopt a step-by-step method to improve accuracy and reliability of the estimated focal parameters as more data become available, ensuring the promptness of the first estimation. Accordingly, Earthquake Early Warnings are disseminated repeatedly with improved accuracy and reliability. This is needed for online control of lifeline systems, railway, factory, emergency action of the citizens, and so on. Furthermore, we are trying to more-rapidly issue tsunami forecasts using Earthquake Early Warning technology.

'Estimated Seismic Intensity' enables seismic intensity estimates for areas where no seismic intensity meter are installed. The calculation flow is as follows.

1) Covert from an observed seismic intensity at the surface to that at the engineering bedrock just below a station by using the amplification coefficient deduced from geology and geography. The amplification coefficient is given at each 1 km mesh across Japan (developed by JMA and the Cabinet Office in cooperation).
2) Interpolate seismic intensity distribution at the engineering bedrock depth.
3) Covert again from the interpolated seismic intensity to that at the surface by multiplying amplification coefficient.

This information is useful to quickly grasp the degree of damage and to plan the effective implementation of a countermeasure just after of the occurrence of a disastrous event.

The Kanto subduction zone: Seismicity, slab deformation and earthquake potential in and around the two subducting oceanic plates

Shin-ichi Noguchi, National Research Institute for Earth Science and Disaster Prevention, 3-1 Tennodai, Tsukuba, Ibaraki, 305-0006, Japan, shin@bosai.go.jp

Deepening our understanding of tectonics in the Kanto subduction zone is particularly important in Japan in order to take various measures to prevent earthquake disasters. Over the past two decades, investigations of hypocenters and focal mechanisms from a number of earthquakes, observed by the development of a seismic network (Okada, 1984), have provided a wealth of information on the geometry of the subducting plates, the stress field and mechanical properties on and around the plate boundaries. Based on the accumulated knowledge and observations, we examine the complex seismicity in the Kanto subduction zone in the framework of the relative movement of three converging plates (Figure 1).

In the Kanto subduction zone, the forearc portion of the young and laterally heterogeneous Philippine Sea plate (PH) subducts beneath the overriding continental plate (the Okhotsk plate, OK, Seno et al., 1996) and descends into the mantle wedge overlying the old Pacific slab (PA, Figure 2). The deeper part of the Philippine Sea slab collides and interacts with the upper boundary of the Pacific slab. The complex distributions of hypocenters and regional variation of focal mechanism solutions are attributed to the compound mode of plate convergence. In particular we can recognize noticeable seismic zones and corresponding stress fields which show local deformation along the two subducting slabs (Figure 3). This deformation is due to the alternation of the contact interface along the PH, PA and OK boundaries. The relative velocity of plate movements, i.e., velocity of OK-PH, OK-PA and PH-PA, are therefore a key to resolve the apparently complex seismotectonics in the Kanto region. Earthquakes can be classified into interplate and intraplate earthquakes for each of these three plates.

The Headquarters for Earthquake Research Promotion recently reported the long-term occurrence potentials of earthquakes in the southern Kanto region. The probability of occurrence of a 1923 type Kanto earthquake is only 0 to 5% during the next 50 years. On the other hand, the probability of the M7 (M6.7-7.2) earthquake, estimated by applying a Poisson process, is 70% during the next 30 years and is 90% during the next 50 years beneath the central and southern Kanto area. At present it is difficult to specify the type and source area of the potential M7 earthquake. Continuous determination of improved hypocenters and focal mechanism solutions, together with information of waveforms, seismic tomography, and seismic reflection and refraction data, are important to define plate boundaries more accurately, and to eventually find the strained area or locked portion along the plate boundaries or within the plates.

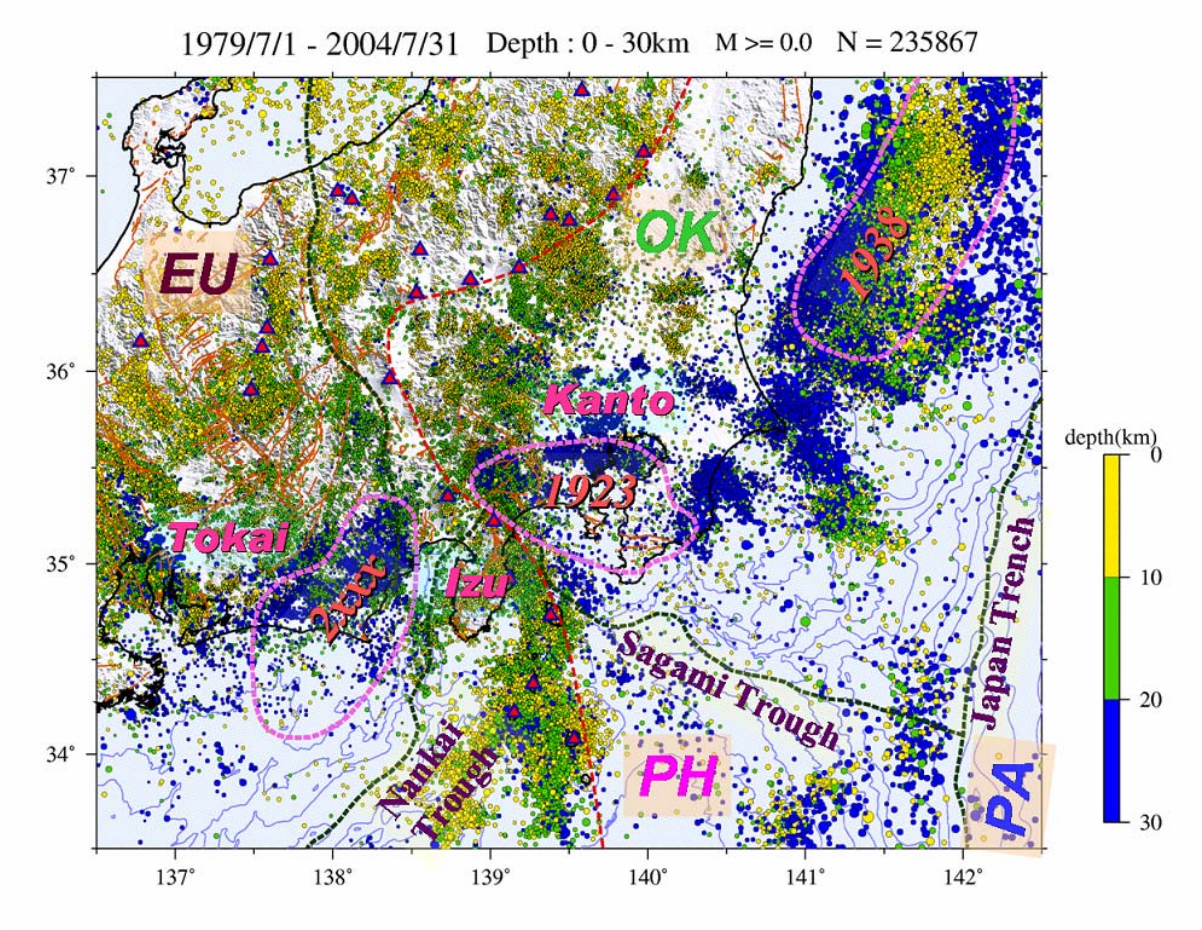

Figure 1 Seismicity of recent shallow earthquakes. Three circled areas are source region of the 1923 Kanto earthquake (M7.9 at OK-PH boundary) and the 1938 Fukushima-Oki earthquake swarms (equivalent to a major M8.1 at OK-PA and within PA), and a hypothetical source area of the next Tokai earthquake (EU-PH), respectively. ISTL: the Itoigawa-Shizuoka tectonic line. Solid triangles: the Quaternary volcanoes.

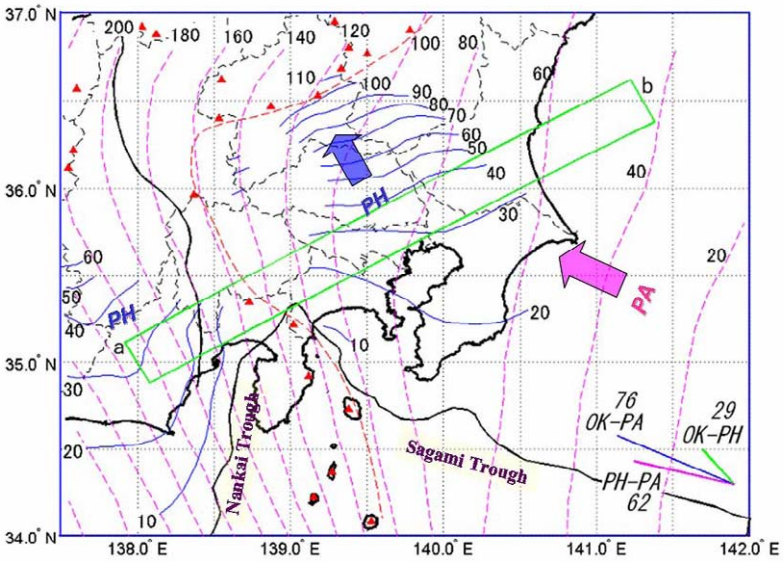

Figure 2 The isodepth contours show the seismic planes of the Pacific plate (PA, dashed lines with 20 km intervals) and the Philippine Sea plate (PH, solid lines with 10 km intervals). Recent seismic tomography suggest the existence of an aseismic slab subducting north of the Izu peninsula, between the Kanto and Tokai slabs (Sekiguchi, 2001). The curvature of the isodepth lines reflect that the hot and young Philippine Sea slab has a heterogeneous and easily deformable structure with less flexural rigidity compared with the old and cold Pacific slab. The relative velocity of plate movement (mm/year) between OK-PH, OK-PA and PH-PA , calculated based on Seno *et al*. (1996) is shown.

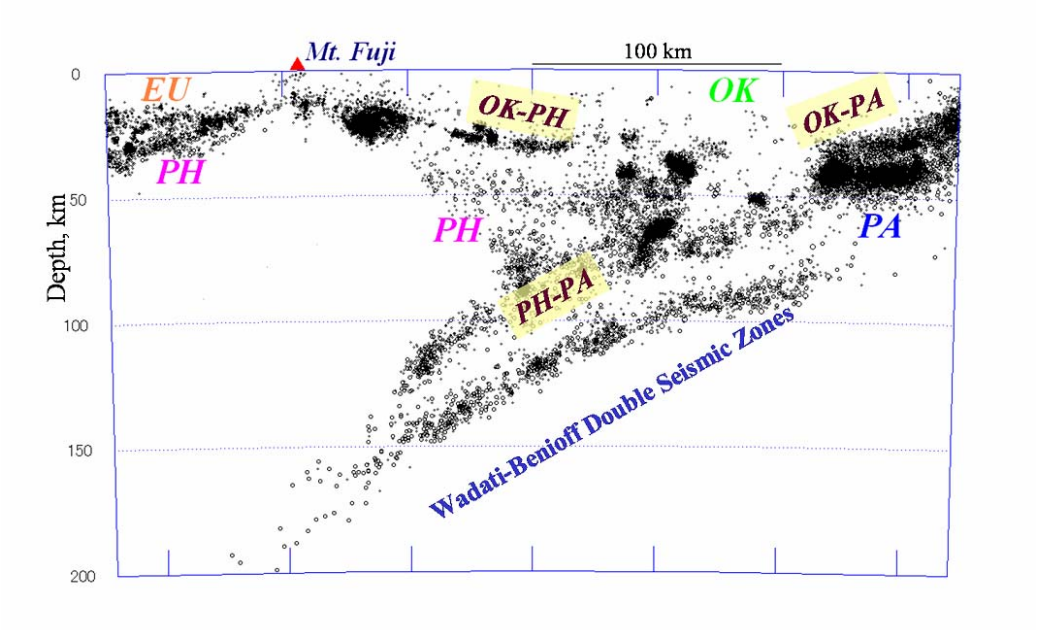

Figure 3 Vertical cross-section of seismicity across the Kanto and Tokai area for the rectangle box ab shown in Figure 2. The relative velocity of plate movements and interactions along OK-PH, OK-PA and PH-PA boundaries may cause local slab deformation or distortion. The intraslab seismic activity can be explained by applying the hypothesis of dehydration embrittlement (Seno *et al*., 2001).

Imaging of the Earthquake Source Fault Beneath the Tokyo Metropolitan Region

Hiroshi Sato[1], Naoshi Hirata[1], Kazuki Koketsu[1], David Okaya[2], Reiji Kobayashi[1], Takaya Iwasaki[1], Tanio Ito[3], Keiji Kasahara[4], Takeshi Ikawa[5], Susumu Abe[5], Taku Kawanaka[5], Makoto Matsubara[4], Steven Harder[6]

1 Earthquake Research Institute, University of Tokyo, Yayoi 1-1-1 Bunkyo-ku, Tokyo, Japan
2 Department of Earth Sciences, University of Southern California, Los Angeles, CA, USA
3 Department of Earth Science, Chiba University, Chiba, Japan
4 National Research Inst. Earth Science and Disaster Prevention, Tennodai 3-1,Tsukuba, Japan
5 JGI Inc., Otsuka 1-5-21 Bunkyo-ku, Tokyo, Japan
6 Department of Geological Sciences, University of Texas El Paso, El Paso, TX, USA

In central Japan the Philippine Sea plate (PSP) subducts beneath the Tokyo metropolitan area where it causes mega-thrust earthquakes, such as the Genroku earthquake of 1703 (M8.0) and Kanto earthquake of 1923 (M7.9) which had 140,000 fatalities. The vertical proximity of this downgoing lithospheric plate is of concern because the greater Tokyo urban region has a population of 33 million and is the center of approximately 40% of the nation's economic activities. A magnitude 7 or greater earthquake in this region at present has the potential to produce devastating loss of life and property with even greater global economic repercussions. In order to reduce such loss in the future the Japanese government began in 2002 the Special Project for Earthquake Disaster Mitigation in Urban Areas, and four seismic reflection experiments have been carried out in the Kanto region to explore the details of the PSP.

We collected four seismic profiles distributed across the greater Tokyo region to optimally image the geometry of the PSP (A-D in Fig. 1) and its asperity zones. Seismic reflections from the top of the PSP are visible in all four profiles. The Neogene-Tertiary accretionary prism is identified in the eastern three profiles. A portion of the Izu-Bonin island arc (TZ) is accreted into the Honshu middle crust via wedge-thrust tectonics. The large-scale fore-arc Kanto basin is present and overlies the upper crustal Honshu pre-Neogene basement (HpN). These profiles image the primary structural features of the overall subduction and two forearc systems within the Kanto region (e.g., schematic cross-sections in Fig. 1).

Seismic reflections of the upper surface of the subducted PSP are observed on all of the seismic sections and are nearly concordant with slab geometry estimated from seismicity (Ishida, 1992). These reflections are found at 5 to 24 km in profile A, 4 to 11 km depths in profile B, and 6 to 25 km in profile C. In the southern portion of profile D, this mega-thrust dips at ~30 degrees from 5 to 20 km depths but exhibits flat geometry towards the north; this apparent flat dip is due to the profile's orientation as a strike line to the locally westward dipping PSP (Fig. 1). A prominent result of this seismic profiling is that the top of the PSP is shallower than has been commonly assumed. Our shallower PSP geometry may lead to a significant intensification in strong ground motion estimations, simply because the cause gets closer to targets. In addition, this geometry serves as a new constraint for studies of Kanto seismotectonics and seismic imaging using earthquakes such as high resolution 3D tomography and receiver function analysis.

Asperities on the PSP mega-thrust represent recent or potential future sources of strong ground motion which have little intervening seismicity. Two asperity zones have been identified based on coseismic geodetic and seismic waveform data and their inversions of the 1923 Kanto earthquake (Wald and Somerville, 1995; Kobayashi and Koketsu, submitted). A

third asperity zone in the Kanto region has been identified via inversion of continuous GPS data for which subsurface slip on the mega-thrust is not keeping pace with surface geodetic movement ("slip deficit") (Sagiya, 2004). These asperity zones represent locked, possible future earthquake sites. Surrounding these three zones under the Kanto region are non-asperity areas characterized by aseismic slip, slow earthquakes, repeating earthquakes and/or greater rates of low-magnitude background seismicity (Sagiya, 2004; Ozawa et al., 2003).

We also note a correlation between the asperities and characteristics of PSP seismic reflections. This relationship has been suggested from observations at the Nankai trough off Shikoku (Kodaira et al., 2000) and Tokai (Kodaira et al., 2004), the Japan trench off Sanriku (Hayakawa et al., 2002), the southern Kurile trench (Nakanishi et al., 2004), Cascadia (Nedimovic et al., 2003), and Barbados (Bangs et al., 1999). The observed relationship between asperity and reflectivity has the potential to locate asperities using seismic profiling.

Bangs, N., T. Shipley, J.C. Moore, G. Moore, 1999, Fluid accumulation and channeling along the northern Barbados Ridge decollement thrust, J. Geophys. Res. 104, 20399-20414.

Hayakawa, T., J. Kasahara, R. Hino, T. Sato, M. Shinohara, T. Kanazawa, 2002. Heterogeneous structure across the source regions of the 1968 Tokachi-Oki and the 1994 Sanriku-Haruka-Oki earthquakes at the Japan Trench revealed by an ocean bottom seismic survey, Phys. Earth Planet. Int., 132, 89-104.

Ishida, M., 1992, Geometry and relative motion of Philippine Sea Plate and Pacific Plate beneath the Kanto-Tokai district, Japan, J. Geophys. Res. 97, 489-513.

Kobayashi, R., and K. Koketsu, 2004, Earth Planets Space, submitted.

Kodaira, S., N. Takahashi, J-O Park, K. Mochizuki, M. Shinohara, S. Kimura, 2000, Western Nankai Trough seismogenic zone: results from a wide-angle ocean bottom seismic survey, J. Geophys. Res. 105, 5887-5905.

Kodaira, S., T. Iidaka, A. Kato, J.-O. Park, T. Iwasaki, Y. Kaneda, 2004, High pore fluid pressure may cause silent slip in the Nankai Trough, Science, 304, 1295-1298.

Nakanishi, A., A. Smith, S. Miura, T. Tsuru, S. Kodaira, K. Obana, N. Takahashi, P. Cummins, Y. Kaneda, 2004, Structural factors controlling the coseismic rupture zone of the 1973 Nemuro-Oki earthquake, the southern Kuril Trench seismogenic zone, J. Geophys. Res. 109, B05305, doi:1029/2003JB002574.

Nedimovic, M., R. Hyndman, K. Ramachandran, and G. Spence, 2003, Reflection signature of seismic and aseismic slip on the northern Cascadia subduction interface, Nature, 424, 416-420.

Ozawa, S., S. Miyazaki, Y. Hatanaka, T. Imakiire, M. Kaidzu, M. Murakami, 2003, Characteristic silent earthquakes in the eastern part of the Boso peninsula, Central Japan. GRL 30, 1283.

Sagiya, T., 2004, Interplate coupling in the Kanto district, central Japan, and the Boso peninsula silent earthquake in May 1996. PAGEOPH 161, 2601.

Wald D. and P. Somerville, 1995, Variable-slip model of the Great 1923 Kanto, Japan, earthquake: geodetic and body-waveform analysis, Bull. Seis. Soc. Am. 85, 157-177.

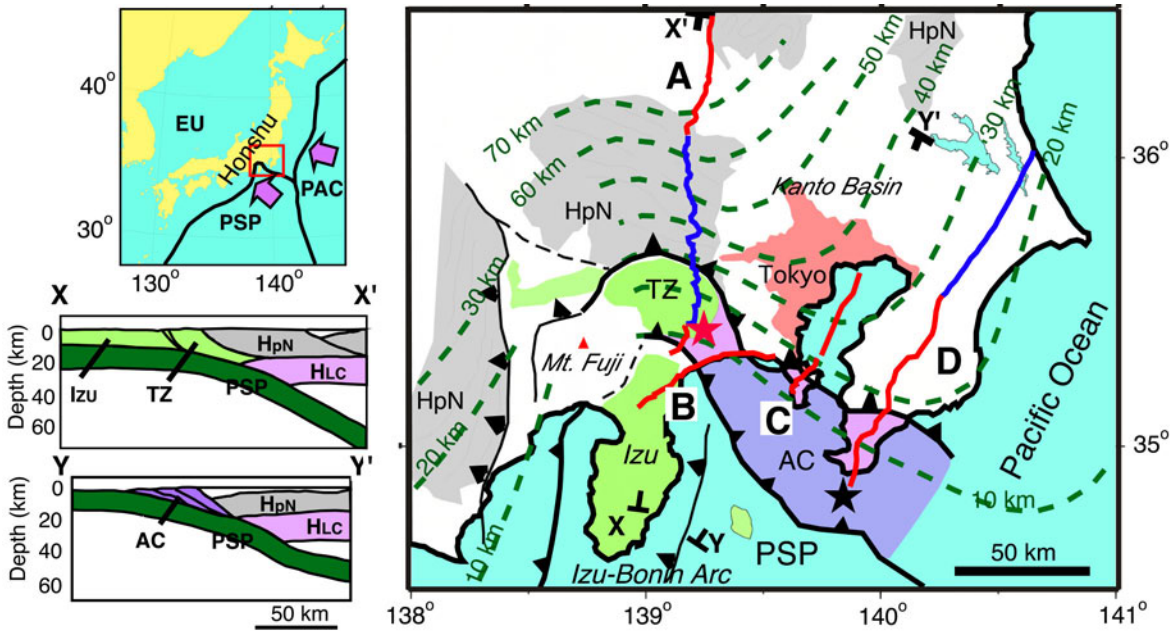

Figure 1. Tectonic region of Metropolitan Tokyo (Kanto) area. (Upper left) Plate geometry of Honshu island. PAC: Pacific plate, EP: Eurasian plate, PSP: Philippine Sea plate. Arrows denote plate convergence directions relative to Honshu. Red box is study area. (Right) Tectonic map of Kanto region and location of seismic profiles A-D. Contours represent depth in km to upper surface of Philippine Sea plate (PSP) from Ishida (1992). Tectonic elements include: HpN: Pre-Neogene rocks belong to Honshu arc, HLC: lower crust of Honshu arc, TZ: Tazawa block (arc fragment of Miocene Izu-Bonin arc), IZ: Izu block, (volcanic Izu-Bonin arc crust), AC: primarily Neogene accretionary complex. Stars are epicenters of 1703 Genroku (black) and 1923 Kanto earthquakes (red). Red and blue profile segments indicate multichannel vibroseis and explosion refraction/wide-angle reflection acquisition methods, respectively. (Lower left) Lithospheric cross-sections across Kanto. X-X' represents arc-arc forearc collision; Y-Y' illustrates accumulation of a standard forearc accretionary complex.

Progress towards a probabilistic hazard analysis for the Kanto region

Ross Stein[1], Shinji Toda[2], William Bakun[1], Masanobu Shishikura[2], Marleen Nyst[1], Takuya Nishimura[3], Fred Pollitz[1], Kenji Satake[2], Yoshimitsu Okada[4], Nobuo Hamada[5], Wayne Thatcher[1], Takeshi Sagiya[6], and Serkan Bozkurt[1]

[1]USGS (rstein@usgs.gov), [2]AFRC, [3]GSI, [4]NIED, [5]JMA, [6]Nagoya University

We are undertaking a collaborative study of the earthquake likelihood for the greater Tokyo area. First, we seek to estimate the time-independent Poisson probability of an earthquake of a given size striking Kanto. Such an assessment rests on the assumption that the historical record is long enough to encompass the full range of earthquake occurrence. We are using new methods to locate and estimate the size of earthquakes. If we can reliably estimate earthquake locations, magnitudes, and their uncertainties, the Poisson probability would reflect the average likelihood of earthquakes striking Kanto over the long term. But it would not necessarily reflect the likelihood during the next decade, which could, in our judgment, depart significantly from the long-term average. This brings us to our second goal:

Second, we would like to build a renewal model of earthquake probability, which treats major faults late in their earthquake cycles as more likely to rupture. Although more demanding than a time-independent assessment, the renewal model is potentially more faithful to the current state of the hazard. Marine terrace data may contain the best evidence for earthquake inter-event times and their variability for Philippine Sea plate events. But we also need to be able to distinguish between upper crustal and subduction historical earthquakes, which depends both on location and depth of events.

Third, we seek to produce what we term an ‘interaction probability’ that explicitly includes the effect of stress transfer to major faults by past earthquakes. There is a change in the distribution of seismicity in the Kanto plain after the 1923 shock, and there also may be a drop in the rate of large events during the century after the 1703 shock. For the interaction probability, we need calculate how the 1923 earthquake elastically stressed faults in its environment, triggering aftershocks and subsequent mainshocks; and how the transient stresses excited by viscoelastic rebound continued to redistribute stress on major faults over the next 50 years.

Thus far, we have completed three studies of the 1923 Kanto earthquake and one on the postseismic deformation. We have developed a new intensity attenuation relation for the Usami and JMA catalogs, and we have developed a new model of strain accumulation to infer the slip deficit on likely seismic sources. For the coseismic and interseismic models, we have been able to greatly augment the geodetic datasets. We are developing a new model of the 1703 Genroku earthquake from coastal coseismic and longterm marine terrace deformation, shaking intensity and tsunami run-up data. We have also created a GIS environment to analyze and visualize the complex 3D tectonic configuration beneath Kanto.

National seismic hazard mapping project of Japan

Hiroyuki Fujiwara, National Research Institute for Earth Science and Disaster Prevention, fujiwara@bosai.go.jp

The Great Hanshin-Awaji Earthquake Disaster on January 17, 1995 killed more than 6,400 people. Following the lessons learned from this disaster, the Earthquake Disaster Management Special Act was enacted in July, 1995 to promote a comprehensive national policy on earthquake disaster prevention. In accordance with this act, the Headquarters for Earthquake Research Promotion was established. In April, 1999, the Headquarters for Earthquake Research Promotion produced 'On Promotion of Earthquake Research – Comprehensive and Fundamental Measures for Promotion of Observation, Measurement and Research on Earthquakes－'. In this article, the Headquarters for Earthquake Research Promotion concluded that preparation of 'National Seismic Hazard Maps of Japan' should be promoted as a major subject of earthquake research. The National Research Institute for Earth Science and Disaster Prevention (NIED) started the special research project 'National Seismic Hazard Mapping Project of Japan' to support the preparation of seismic hazard maps made by the Headquarters for Earthquake Research Promotion in April, 2001. The National Seismic Hazard Maps of Japan consist of two types. One kind of hazard map is a probabilistic seismic hazard map that shows the relation between seismic intensity value and its probability of exceedance within certain time period. The other kind of hazard map is a seismic hazard map with a specified seismic source fault. This type of hazard map is sometimes called a scenario earthquake shake map. As the first step in preparations for producing the seismic hazard maps, which are scheduled to be completed by the end of fiscal year 2004, preliminary versions of probabilistic seismic hazard maps for the Northern part and the Southwestern part of Japan and scenario maps for several earthquakes, e.g. earthquakes in Itoigawa Shizuoka tectonic line fault zones, Miyagi-ken-oki earthquakes, have been prepared. I present the outline of the methodologies used to evaluate spatial strong-motion distributions both for the probabilistic seismic hazard maps and for the scenario earthquake shake maps.

For the probabilistic seismic hazard maps, we use empirical attenuation relations for evaluation of strong-motion. It is difficult to adopt simulation methods based on source modeling such as the hybrid method because the simulation methods need too much computation to evaluate spatial distributions of strong-motion for all possible earthquakes. For the scenario earthquake shake maps, however, we can adopt the simulation method based on the source modeling. The hybrid method is adopted as the simulation method for strong-motion evaluation. The hybrid method aims to evaluate strong-motions in a broadband frequency range and is a combination of a deterministic approach using numerical simulation methods, such as the finite difference method (FDM) or the finite element method (FEM), for a low frequency range and a stochastic approach using the empirical or stochastic Green's function method for a high frequency range. A lot of information on source characterization and modeling of underground structure is required for the hybrid method. The standardization for setting parameters of the hybrid method is studied in the National Seismic Hazard Mapping Project. The technical details on the hybrid method are summarized in 'Recipe for strong-motion evaluation of earthquakes in active faults' and 'Recipe for strong-motion evaluation of earthquakes in plate boundaries', which are published by the earthquake research committee of Japan. Characterized source models are composed of asperities and a background slip area surrounding the asperities. Source parameters required to evaluate strong-motions by using the characterized source model are classified into three parts. The first part is the set of outer parameters that show the magnitude and the fault shape of the earthquake. The second part is the set of the parameters that describe

the degree of fault heterogeneity. The third part is the set of the parameters to define the characteristics of the rupture propagation. The selection of a specific earthquake is essential to make a scenario earthquake map. The basic policy of the selection of a scenario earthquake in the National Seismic Hazard Mapping Project is that we choose the most probable case. However available information to determine the source parameters of the scenario earthquake is often insufficient, but a decision even without complete information is often required. When we do not have sufficient information, we test several cases of the characteristic source model and compare their results to show deviation of strong-motion evaluation due to uncertainties. In order to improve the accuracy of the hybrid method, we must develop new computer capacities and simulation techniques, improve modeling of the rupture processes, and perform advanced modeling of underground structures.

USGS Earthquake Hazards Program in Northern California – Probabilities to Prediction

Mary Lou Zoback, U.S. Geological Survey, Menlo Park, CA 94025, Zoback@usgs.gov

USGS earthquake hazard research in northern California is focused on defining the likelihood of future earthquakes ("probabilities") and anticipating and defining the effects and consequences of those earthquakes ("prediction") of likely shaking, liquefaction, and landslide hazards. New hazard products are being developed and fundamental research is being carried out. Regarding products, a recent comprehensive analysis lead by the USGS concluded that the greater San Francisco Bay region has a 62% likelihood of a major damaging earthquake (M6.7 or greater) over the next 30 years. A series of prototype urban hazard maps (including deterministic shaking, earthquake-triggered landslide, and liquefaction hazard, as well as non-seismic landslide susceptibility) have recently been completed for the city of Oakland, a city with a complex distribution of young, poorly consolidated sediments and which sits astride one of the most hazardous faults in the region, the Hayward fault. Current efforts are focused on producing several major products for the 100th anniversary of the 1906 San Francisco earthquake: 1) a 3D structural representation and slip characterization of the Quaternary faults throughout the greater San Francisco Bay region 2) a unified, correlated map of Quaternary deposits mapped at 1:24,000 and a derived liquefaction susceptibility map utilizing Holocene thicknesses and depth to groundwater, and 3) simulation of 1906 ground motions utilizing a new source-time function for 1906 and a new 3D velocity model that will include faults and fault blocks.

Collaborative SCEC/USGS Efforts to Improve Seismic-Hazard Analysis: RELM and OpenSHA

Edward (Ned) H. Field, U.S. Geological Survey, Pasadena, CA, field@caltech.edu

There is consensus that significant improvements in seismic-hazard analysis (SHA) will require a more physics-based approach to modeling. In addition, proper SHA requires that all viable earthquake-forecast and ground-motion models be accounted for in the analysis (to adequately represent epistemic uncertainties). Unfortunately, our community has lacked an SHA computational infrastructure capable of handling the wide variety of models currently under development, especially those that are more physics based. To help remedy this situation, there are two ongoing collaborative efforts between the USGS and the Southern California Earthquake Center (SCEC): RELM and OpenSHA.

RELM stands for the working Group for the development of Regional Earthquake Likelihood Models (http://www.RELM.org). The goal is to develop a variety of viable, earthquake-rupture forecast models (rather than one consensus model). We also plan to formally test each model against available geophysical observations, as well as evaluate the seismic hazard implications. The models currently under development range in sophistication from simple Poisson models (e.g., based on smoothed historical seismicity) to physical earthquake simulators that track stress changes throughout the system.

OpenSHA (http://www.OpenSHA.org) is an object-oriented, open-source, and web-based "community-modeling environment" for SHA. The goal is to enable any arbitrarily sophisticated (e.g., physics based) model component to "plug in" without having to change what is being plugged into; that is, without rewriting existing code. This infrastructure allows the models, as well any data repositories upon which they depend, to be geographically distributed and run-time accessible over the Internet. Building such a community-modeling environment has raised several issues related to computational speed, ease of use, error prevention, and repeatability of results in an environment where the models and data are continually being updated. The SCEC Information-Technology Research collaboration is helping resolve some of these issues.

From isolated sites to complete ruptures; the next hurdle for paleoseismology on the southern San Andreas fault

Weldon, R., University of Oregon, ray@newberry.uoregon.edu
Biasi, G., University of Nevada, Reno
Fumal, T., USGS-Menlo Park
Scharer K. University of Oregon

At least fifteen sites on the southern San Andreas fault provide some information on the timing or displacement of large earthquakes. This data is often sufficient to determine a mean recurrence interval, the time interval since the most recent earthquake, and crude estimates of magnitude. Unfortunately, the wide range of ages, recurrence intervals and displacements seen from site to site preclude any simple correlation of site specific information into compelling rupture sequences. We illustrate the variability of possible rupture sequences by constructing a series of rupture scenarios. For example, in (A) ruptures are interpreted as similar-length quasi-periodic northern or southern fault earthquakes with substantial overlap and the 1812 event is anomalous. By contrast (B) is a fairly random distribution of lengths and intervals with highly variable overlap, recurrence intervals, and lengths. In the talk we will speculate about what breakthroughs in data and interpretation will be needed to generate unique paleoruptures for the southern San Andreas fault.

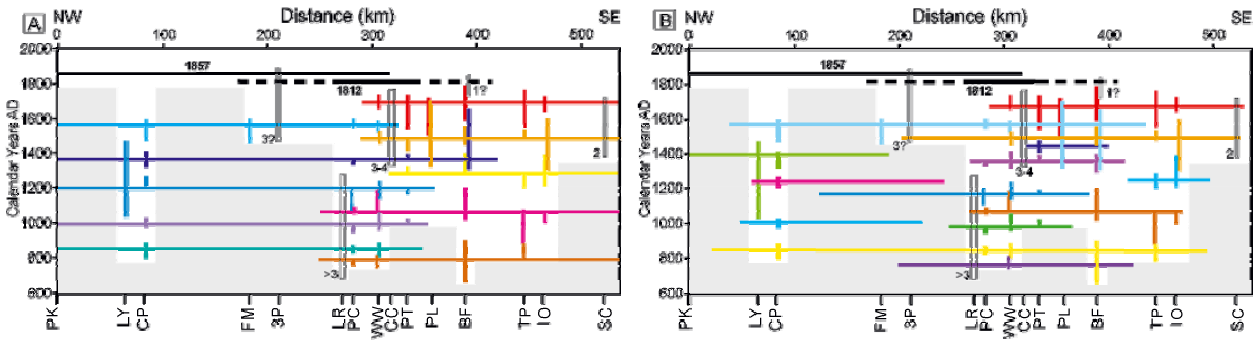

Figure 1. Vertical colored bars are age ranges for sites listed at the lower margin and horizontal bars are hypothetical ruptures. Gray shading indicates regions and times with no data and open boxes represent multiple event age ranges.

Recent progresses in active fault researches and paleoseismology in Japan

Eikichi Tsukuda, Yuichi Sugiyama, Yasuo Awata and Toshikazu Yoshioka
Geological Survey of Japan, AIST, e-tsukada@aist.go.jp

The Active Fault Research Center (AFRC), of the Geological Survey of Japan/AIST plays a major role in the study of active faults and paleoseismology in Japan. Of the 98 major active faults in Japan, AFRC has studied 40 since the 1995 Kobe earthquake. Using various geological methods such as geologic mapping, trenching, boring and seismic profiling, some of the main parameters were obtained. The fault extent, geometry, slip per event, and slip rate are important factors in paleoseismology and the segmentation of each fault. These data are used for evaluation of active faults by the Earthquake Research Committee of Japan.

AFRC is also constructing a comprehensive active fault database according to the same standard. These data will be used to make a probabilistic evaluation of future faulting events and earthquake occurrence on the major active faults in Japan. The database consists of three sub-databases, (1) a sub-database on individual sites, which including long-term slip and paleo-faulting data with error range and reliability, (2) a sub-database on the details of paleo-faulting, which includes the excavated geological units and faulting event horizons with age-control, and (3) a sub-database on the characteristics of behavioral segments, which includes the fault length, long-term slip-rate, recurrence interval, most-recent event, slip-per-event and best estimated segment for cascade earthquakes. Active faults in Japan are segmented into about 550 behavioral segments based on the geometry of the fault strand separated by discontinuities of larger than 2-3 km, and timing of paleo-faulting and slip-rate. Those behavioral segments are re-structured into approximately 330 "seismogenic faults", which are probably the best-estimation for large earthquake segments, separated by jogs larger than 5 km. 290 segments were evaluated in detail, with 150 major segments having length >= 20 km and >= 0.1 m/ky in long-term slip-rate. Based on the standardized data, we evaluate the possibility of future rupture, and the earthquake magnitude for each fault, taking into account single- and multiple-segment earthquakes.

For example, the 1891 80 km-long Nobi earthquake rupture consists of three behavioral segments which are the Nukumi, Neodani and Umehara segments, and two other behavioral segments with less than 10 km in length. The 23-km-long Nukumi segment is evaluated to have a slip-rate of 1.2 m/ky, slip per event of 2.7 m and recurrence interval of 2342 years. The 36-km-long Neodani segment has a slip-rate of 1.9 m/ky, slip per event of 4.9 m and recurrence interval of 2615 years. The 27-km-long Umehara segment has a slip-rate of 0.1 m/ky, slip per event of 2.2 m and recurrence interval of about 22000 years. In addition, a part of the "seismogenic segment" consists of two behavioral segments not ruptured during the 1891 earthquake.

The number of behavioral segments in a single seismogenic fault varies between 1 and 14, with an average of approximately 2. The length of each segment averages about 20-25 km and only several segments are longer than 45 km. The longest seismogenic faults, namely the 350-km-long Median Tectonic Line Active Fault System was probably ruptured during the 16th century, in a series of large earthquakes, and the second longest Itoigawa-Shizuoka Tectonic Line Active Fault System was also ruptured between the 8th and 9th centuries. These average number and length of most of the segments are almost the same as the behavioral segments of surface ruptures that occurred in Japan since 1891. Displacement per event of the segments varies between one and several meters, and does not show significant regional variation. The amount of displacement is not a function of the length of the seismogenic fault, but of the

behavioral segment. On the other hand, the recurrence interval for faulting events on those segments varies very much from 1 ky to 30 ky or more. The interval has a tendency of increasing from the outer arc side to the inner arc side on land, according to the gradient of crustal strain in both geological and geodetic times.

In the course of this study, we chose the Uemachi fault for precise survey and application to strong motion evaluation. The Uemachi fault is a 45-km-long blind thrust fault, beneath metropolitan Osaka, central Japan. The entire rupture of the fault would cause an M7 earthquake right under the urban area. The maximum 30-year earthquake probability of the fault is estimated to be 3 %, which is nearly the same as the Nojima fault, a causative fault of the Kobe earthquake. We made several possible geometrical models for the Uemachi fault including one-segment and two-segment models, and estimated heterogeneous coseismic slip distribution (asperities) from the geologically-obtained uplift rate distribution. The slip distribution is converted into static stress change, which is then incorporated into dynamic rupture simulation as a variation of initial stress. The simulation shows that the rupture area depends on fault geometry and initial crack location. Because Osaka is located in a deep Quaternary sedimentary basin, an accurate structure model is necessary for precisely predicting ground motions. A 3D basin structure model was constructed based on geological and geophysical data obtained by deep boreholes, seismic reflections and gravity measurements. Medium constants such as S-wave velocity are given to each grid point at 100 m horizontal and 50 m vertical intervals. Geometry of key beds and fault-related structural discontinuities are realistically expressed. Ground motions up to 1 Hz were computed in the 3D Osaka basin structure model by the 3D finite difference method. The heterogeneous initial stress drop controls the simulated rupture process and the effect is directly reflected in the computed ground motion distribution. Long (~10km) -wavelength heterogeneity in the rupture process can be deterministically constrained by active fault data, but shorter wavelength heterogeneity needs to be estimated by other data or modeled stochastically.

Long-Term Paleoseismic Earthquake Records along the Cascadia Subduction Zone and Northern San Andreas Fault based on Turbidite Stratigraphy

Chris Goldfinger[1], C. Hans Nelson[2,3], Joel E. Johnson[1,4], Jason D. Chaytor[1], Eugene Karabanov[5], Andrew Eriksson[1], Ann Morey-Ross[1], and Shipboard Scientific Parties 1999 and 2002

[1] Oregon State University, Corvallis, Oregon. gold@coas.oregonstate.edu
[2] U.S. Geological Survey, Menlo Park, CA
[3] Now at Instituto Andaluz de Ciencias de la Tierra, Granada, Spain odp@ugr.es
[4] Now at Monterey Bay Aquarium Research Institute, Moss Landing, CA
[5]University of South Carolina, Geology Department Columbia, SC

We have been investigating the recurrence pattern of Great Earthquakes along the Cascadia and Northern San Andreas margins using the record of abyssal plain turbidites. In Cascadia, we have previously suggested that virtually all turbidites record great earthquakes, based on identical numbers of events in widely separated cores, and relative dating techniques that demonstrate synchroneity of the triggering mechanism. The correlation used thus far has relied upon the presence of the Mazama ash in most cores. We have additionally tested this correlation with radiocarbon ages and physical properties of the core sediments. Despite a systematic spatial and temporal variation in 14C reservoir ages, we find that the repeat pattern of events supports regional correlation. We find also that a good stratigraphic correlation can be made between three key core sites at Juan de Fuca, Cascadia, and Rogue Channels using Gamma density and high-resolution magnetic susceptibility records of these cores. This correlation is independent of other correlation methods including the Mazama ash datum, event number comparisons, the "confluence test" of synchronous triggering, and radiocarbon ages, but is consistent with them. That we are able to correlate physical property "wiggle" plots between turbidite channels that are not connected, implies that something of the earthquake shaking signal may be contained in these records. With strengthened correlations, and improved estimates of the reservoir correction, we infer that the pattern of Cascadia Great Earthquakes appears to include a repeating pattern consisting of a long interval ending in an earthquake, followed by a moderately long interval, then 1 or 2 shorter intervals. Over the last ~9000 years, the pattern appears to have repeated four times.

Northern San Andreas work is in progress, using similar methods to correlate events between channels, establish an event chronology with 14C and hemipelagic thickness data, and use multiple confluences to test for synchronous triggering of events.

Importance of the geological investigations for paleoseismology in areas with short history

Takashi Azuma, Active Fault Research Center, Geological Survey of Japan/AIST,
t-azuma@aist.go.jp

Earthquake scientists study previous earthquakes and present seismological data for the purpose of predicting large earthquake in the future. There are several methods for researching previous earthquakes with different time-scales and accuracy. Seismological and geodetic methods make precise and detailed data for the short period (less than 100 years), whereas historical, topographic and geological methods yield evidence of previous earthquakes during the long term (100-100,000 years). On the other hand, there is a fundamental rule that the larger earthquake occurs less frequently. The interval period for the occurrence of the large earthquakes in a certain area is on the order of 100 years for the interplate earthquake and 1000-10,000 years for the intraplate earthquakes generated from active faults. Therefore seismological and geodetic methods can not cover the whole intervals of large earthquakes, and other methods should also be used for the prediction of these large events.

The historical method is useful for areas where the historical records are well-preserved, such as the Kinki region in western Japan. Some official reports or private diaries document the date of large earthquakes and the damage associated with them. However, there are many areas lacking in long historical records. For example, the native people in Hokkaido, northern part of Japan Islands, have an oral culture, thus there are no documents prior to the 17th century in that area. In the offshore of Hokkaido, there is a subduction-zone along the Kuril trench and several active faults are distributed in this area. For this area, topographic and geological methods can be useful to identify the large earthquakes with long intervals.

In a recent study, our group surveyed one of the active faults in Hokkaido, called the Kuromatsunai-teich fault zone. This fault zone is 25 km length and has the potential for producing M7.3 earthquakes. We found the last event on this fault zone was about 5,500 years ago. The frequency of occurrence on this fault is low, but it is important to observe the active fault because the earthquake was generated at shallow depth, and was close to an inhabited area. It is also important to study the simulation of the strong ground motion and the estimation of displacement near the active fault.

On the Pacific coast of eastern Hokkaido, the timing of previous large earthquakes and their magnitude was determined by detailed study of the tsunami deposits. From the results of this study, an anomalous earthquake with a prominently, large tsunami was found (Nanayama et al., 2003). This large earthquake was about 500 years ago, and the inundated area was much wider than normal plate boundary earthquakes with a 100-150 year interval. This anomalous earthquake seemed to be generated from the multi-segment interplate rupture.

Despite their usefulness, topographic and geological methods have many uncertainties. For example, it is difficult to separate multiple events within several years, because the resolution of these methods is much lower than other methods. Furthermore, many moderate earthquakes cannot be recognized by geological evidence alone. We should therefore survey for large and infrequent earthquakes with intervals of more than 100 years by using topographic and geological methods, while paying attention to the weakness of the method.

Thrust Faults in Transpressive Strike-Slip Environments—Role of the Susitna Glacier Fault in the M_w 7.9 Denali Fault Earthquake Sequence, Alaska

Anthony J. Crone[1], Stephen F. Personius[1], Patricia A. Craw[2], Peter J. Haeussler[3], Lauren A. Staft[2]

1 U.S. Geological Survey, Denver, Colorado, crone@usgs.gov
2 Alaska Division of Geological and Geophysical Surveys, Fairbanks, Alaska
3 U.S. Geological Survey, Anchorage, Alaska

The 3 November 2002 M_w 7.9 Denali fault earthquake produced 341 km of surface rupture on three faults in central Alaska. The earthquake was comprised of at least three subevents. Thrust faulting on the previously unrecognized Susitna Glacier fault started the earthquake sequence and generated the initial M_w 7.2 subevent. We mapped 48 km of surface rupture on the Susitna Glacier fault; the surface faulting formed scarps on ice of the Susitna and West Fork glaciers and on surficial deposits along the southern front of the central Alaska Range. The 2002 surface faulting produced structures that range from simple folds on single traces to complex thrust-fault ruptures and pressure ridges on multiple, sinuous strands that are locally more than 1 km wide. We measured a maximum vertical displacement of 5.4 m on the south-directed main thrust, and locally, vertical displacements of more than 4 m on north-directed backthrusts. Typical vertical displacements on the 2002 ruptures are 1-3 m. We measured a well-constrained near-surface fault dip of about 19° at one site and 10° at a second site. Both of these surface measurements are considerably less than seismologically determined values of 35-48°, which suggests that the fault plane is flattening near the surface.

The Susitna Glacier fault was the nucleation point for the larger M_w 7.9 earthquake sequence, and thus highlights the importance of understanding the role of active thrust faults in partitioning strain in transpressive tectonic environments. Comparison of our field and the seismological data suggest that the Susitna Glacier fault is part of a large positive flower structure associated with northwest-directed transpressive deformation on the Denali fault. Late Cenozoic movement has been reported on other reverse faults in the region, but it is poorly documented. Because the tectonic geomorphology of the range front in the vicinity of the Susitna Glacier fault is not distinctive nor is the topography unusually high compared to other parts of the Alaska Range, we suspect that other unrecognized but potentially active thrust faults may be present on both the north and south margins of the Alaska Range. These unrecognized faults could intersect existing or future transportation and pipeline corridors and could contribute significantly to the region's seismic hazard.

A full assessment of the seismic hazards associated with major transpressive strike-slip fault systems such as the Denali and San Andreas faults requires an understanding of the interaction between master strike-slip faults and secondary thrust faults. Paleoseismology can provide unique insight into this interaction by documenting the times of past ruptures on individual faults. The presence of prehistoric scarps along the Susitna Glacier fault shows that it has probably ruptured in late Holocene time, but more detailed work is needed to determine if past movements on the Susitna Glacier fault have repeatedly coincided with ruptures on the Denali fault. Ongoing studies suggest that the recurrence time for surface ruptures on the Susitna Glacier fault may be measured in thousands of years versus hundreds of years for the main Denali fault. Paleoseismological studies of the Denali fault and associated active thrust faults in the region will provide insight into the interaction and behavior of faults within the entire transpressive strike-slip system.

Earthquake Geology of the Denali Fault System, Alaska

David P. Schwartz [1] , Peter J. Haeussler [2] , Ari Matmon [1] , Timothy E. Dawson [3] , Gordon Seitz [4] , Heidi Stenner [1] , Sean Bemis [5] , Emily Molhoek [5] , Brian Sherrod [6] , Anthony J. Crone [7] , Steven Personius [7] , Patricia Craw [8] , Jim Beget [5]

(1) USGS, Menlo Park, dschwartz@usgs.gov (2) USGS, Anchorage, (3) USGS contractor, (4) San Diego State University, (5) University of Alaska, Fairbanks, (6) USGS, Seattle, (7) USGS, Golden, (8) DGGS, Fairbanks

The M7.9 Denali fault earthquake of November 3, 2003 was the largest shallow crustal event in North America since the 1906 rupture of the San Andreas fault. It was produced by 341 km of surface rupture along the Susitna Glacier thrust fault (see Crone et al, this volume) and the Denali and Totschunda strike-slip faults. The 2002 earthquake renewed interest in this fault system, which had remained essentially unstudied since pioneering investigations in 1973 for the Trans-Alaska pipeline. Our new efforts are aimed at developing an understanding of how this large strike-slip and thrust system works in time and space through a) paleoseismic recurrence data, b) slip rates from cosmogenic isotope dating of long-term offsets, and c) paleo-offset information. The slip distribution for the 2002 event is central to interpreting the behavior of this fault.

Immediately following the 2002 earthquake, a reconnaissance team mapped the extent of surface faulting, and developed a preliminary slip distribution (see Eberhardt-Phillips, 2003). In the summer of 2003 we returned to the fault to refine the slip distribution by increasing the number of offset measurements and re-measuring important localities made under snow cover in November 2002. The detailed results are described in Haeussler et al (in press, 2004). Figure 1 shows the offset values used in our interpretations (open circles 2002, black dots 2003); the shaded area is the slip distribution defined as the envelope of maximum slip values. We also developed slip distributions using the same measurements with a) a 5km running average and b) a graphical fit. These different approaches yield average surface slip for the entire rupture (including the Susitna Glacier fault) of 4-4.5m .The three methods of calculating average surface slip all yield a moment magnitude of M_w7.8, which is in very good agreement with the seismologically determined magnitude of **M**7.9 and indicate that surface slip is representative of slip at depth. A comparison of strong motion inversions for moment release with our slip distribution shows they have a similar pattern. The locations of the two largest pulses of moment release correlate with the locations of increasing steps in the average values of observed slip. This suggests that data on slip distributions data can be used to infer locations of large moment release along other active faults.

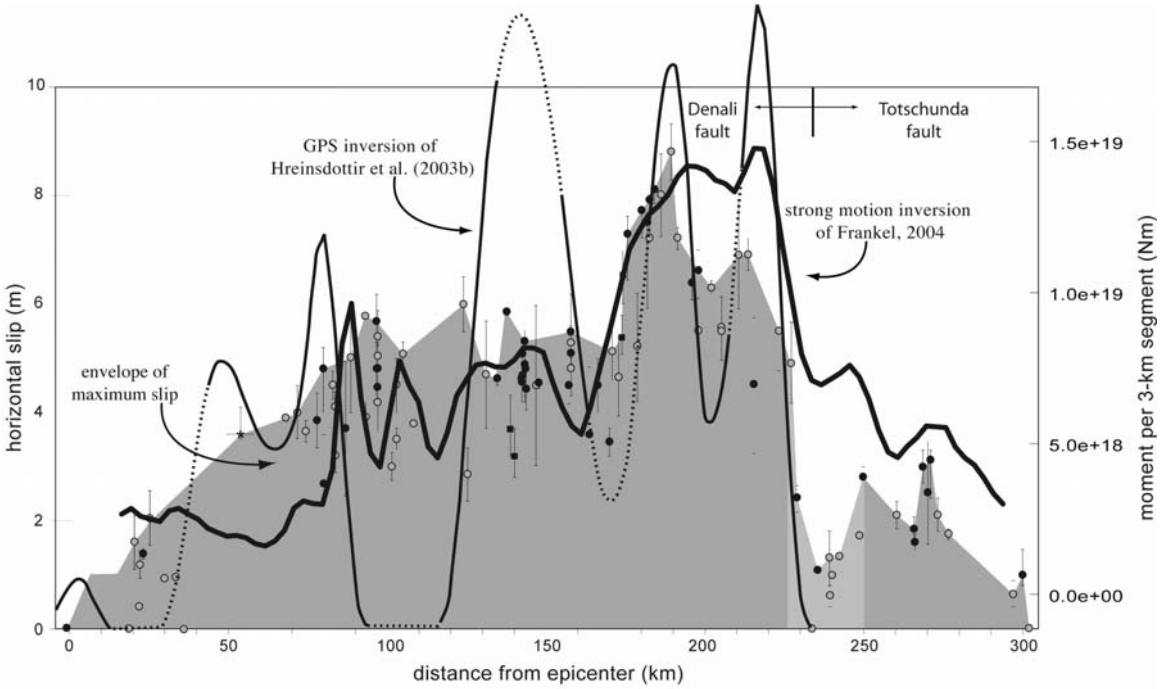

Figure 13.

Figure 1. Comparison of surface slip distribution (from envelope of maximum slip) to strong-motion and geodetic models of moment release along the Denali and Totschunda faults. Thick black line shows strong motion inversion of Frankel (2004). Thin black line shows GPS geodetic inversion of Hreinsdóttir et al. (2003b); dashed where the inversion is poorly constrained. Vertical scale for strong-motion inversion of Frankel (2004) is shown on the right. (From Haeussler et al, in press 2004)

As part of the 2003 field work we took advantage of natural exposures of the fault, primarily transtensional pull-aparts and fault parallel fissures, to identify and develop estimates of the ages of earthquake event horizons. The Denali fault system is a "radiocarbon paradise" with deposits along the fault datable by peats, buried trees, and buried fragile features such as spruce needles locally preserved by permafrost. In 2003 preliminary estimates of event ages were developed at sites on the Denali and Totschunda ruptures. In addition, a campaign was initiated to obtain long-term (late Pleistocene-Holocene) slip rates along all components of the fault system through Al^{26} and B^{10} cosmogenic isotope dating of offset piercing points, mainly glacial moraines. Slip rates along the entire fault system, in conjunction with the 2002 slip distribution, are a major basis for interpreting its behavior.

In the summer of 2004 we expanded the recurrence and slip-rate studies. In addition to refining our initial evaluations of event horizons, sites were examined on the west end of the 2002 rupture and on the unruptured western and eastern Denali fault segments. Information on the timing of the most recent event (MRE) on the unruptured fault sections is required to evaluate the potential impact of stress changes from the 2002 event and time dependent hazards. The 2004 trenches were excavated by hand. Figure 2 is an example of one of these, a trench across the unruptured eastern segment of the Denali fault.

Figure 2. Photo of trench across the eastern unruptured Denali fault. The trench is 2m deep. Radiocarbon samples were collected during reconnaissance in July 2004 and dated prior to more extensive trenching in August 2004. Note broader zone of deformation at depth and rupture (orange flags) and the most recent event (red flags) extending to near the surface.

Paleoseismic Observations

Our field efforts to date are summarized on Figure 3. We now have eleven sites for paleoearthquake dates. These will provide timing of the MRE and penultimate events for the entire fault system, and at some locations will give a three to four event chronology. Three sites are along the Totschunda fault and expose two events prior to 2002. There are four sites on the main 2002 Denali fault rupture; these also expose the two events prior to the 2002 rupture. The eastern unruptured Denali site has evidence of the past three, and possible four, paleoearthquakes. The sites on the western unruptured Denali will provide the timing for the MRE and penultimate event. The timing of the penultimate earthquake will be obtained on the Susitna Glacier thrust (Crone et al., this volume).

Preliminary radiocarbon constraints on earthquake event dates are shown (in black) on Figure 3. The previous large event(s) (slip similar in amount to 2002) on the 2002 Denali and Totschunda ruptures occurred 450-650 years ago. With the present limited dating it is uncertain if these were one or distinct events, but additional dating should resolve this. The pre-penultimate event on the Denali appears to have occurred about 900 years ago, and on the Totschunda about 1200 years ago.

The MRE on the eastern unruptured Denali fault post-dates a paleosol with wood dated at 570-720 yr before 2002 (Figure 2). This rupture extends essentially to the surface and it is likely to be younger than the MRE on the Totschunda fault. A paleo offset from the MRE of 1.5 m was measured 15 km east of the site. We hope that samples collected in 2004 will allow us to determine if the eastern Denali ruptured in conjunction with the penultimate Denali event or was independent.

The western unruptured Denali fault is characterized by extremely youthful geomorphology. Between the west end of the 2002 rupture and the Parks Highway the MRE displaces all deposits and surfaces with fresh and angular scarps, graben, en echelon ruptures, and moletracks. We observed gully offsets of 8m that clearly represent multiple events and a site with 4m offsets for the MRE. We feel the most recent large event along this part of the Denali is very young, and qualitatively place it at less than perhaps 250 years.

A section of the fault from about the Richardson Highway to 30km west of the west end of the 2002 rupture is associated with a broad left (transpressional) bend in the fault, the low slip section of the 2002 strike-slip rupture, and the Susitna Glacier thrust. The western 50 km are characterized by geomorphically young offsets of 1-1.5m. Gary Carver and George Plafker (personal communication) recently concluded that trees damaged by the 2002 rupture near the Delta River were previously damaged from surface rupture in 1912. On the basis of felt intensity data from the 1912 earthquake they suggest this rupture propagated westward. Whether the 1-1.5m offsets are from the proposed 1912 earthquake or are the eastern tail of a large western Denali fault rupture are presently uncertain. Our trench site located 18 km east of the 2002 epicenter exposes the penultimate event and provides a test for the possible westward extent of the proposed 1912 earthquake rupture.

Initial observations indicate that the Susitna Glacier thrust fault fails less frequently than the strike-slip Denali (Crone et al., this volume).

Slip Rate

Figure 3 shows localities where long-term offsets have been measured and sampled for cosmogenic isotope dating. Presently there are ten localities that will provide slip rates. The amount of offset at each location, which ranges from 64m to 300m, is shown in black. Initial results from our 2003 work (Matmon et al, 2004) yield rates of 11.4 mm/yr (for the past 12.3ka) and 12.2 mm/yr (for the past 14.1ka) for the Denali fault. At these locations slip in 2002 and the penultimate event averaged 5m/event. The preliminary slip rate on the Totschunda fault is 8.9 mm/yr (for the past 16.6ka); 2002 and the penultimate offset at this location averaged 3m. Sites sampled in 2004 will extend slip rate coverage to the entire fault system.

Figure 3. Locations of paleoseismic and slip rate sites on the Denali fault system, 2003 and 2004.

Summary

The Denali fault system with its recent large rupture, widespread distribution of preserved organic deposits for radiocarbon dating, extremely well-preserved fault geomorphology, and paleo-offsets is a natural laboratory for studying the behavior of large strike-slip faults on a variety of time scales. Comparisons to the San Andreas fault system, particularly to the southern San Andreas, are obvious. Understanding the longer term rupture history of the Denali fault has implications for seismic hazards in Alaska, fault segmentation, and time-dependent earthquake hazards mapping.

A preliminary model for the Denali fault suggests that: 1) there are two discrete large-slip rupture segments that repeat with similar-sized offsets. These are the Denali section of the 2002 rupture and the western Denali fault; 2) the large rupture segments may overlap in a zone that also produces smaller, independent earthquakes (1912?); 3) the Totschunda and easternmost Denali can fail in concert with the main Denali and also independently; and 4) the Susitna Glacier fault does not rupture as often as the Denali fault. This model will evolve as additional event horizons are observed and radiocarbon dates are obtained. Observations indicate there are locations along the fault system that have the potential to yield long earthquake records.

New GEONET system - Japanese dense GPS observation network for crust monitoring

Atsushi Yamagiwa, Geographical Survey Institute, Japan, yamagiwa@gsi.go.jp

The GPS Earth Observation Network system (GEONET) of the Geographical Survey Institute (GSI) has been playing an important role in monitoring the crustal deformation of Japan. Since the start of its operation, the requirements for accuracy and timeliness have become more imperative. In early 2003, GSI upgraded the GEONET system to meet new requirements. In this presentation, we introduce the new GEONET system and its achievements and potential for crust monitoring.

(1) Reinforcement of the network

The number of the GEONET stations was increased to 1200 by adding 253 new stations (Figure 1). The new sites include the Minamitorishima Island (Marcus Island), which is at the eastern end of Japanese territory and the only island of Japan on the Pacific plate. The choke ring antennas of Dorne Margolin T were adopted, the antennas of the existing stations were also replaced with this type. The seismic observations are recorded at a 1 Hz sampling rate.

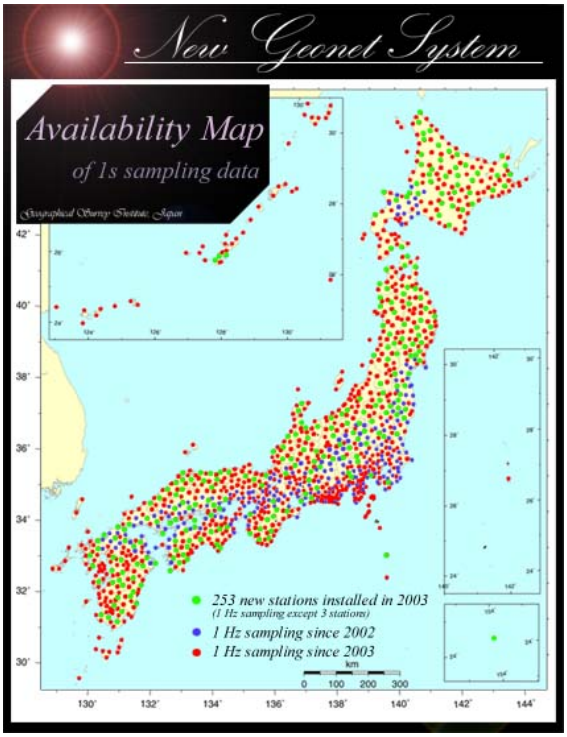

Figure 1. Distribution map of GEONET stations

(2) Real time data transmission

The observed data of all stations, with several exceptions, are transferred in real time through the IP/VPN network. The 1 Hz data are also provided to commercial users for positioning service. The 1 Hz data are decimated in to 30-second interval and stored in the database in GSI (Figure 2, see also Figure 1).

(3) Enhancement of routine analysis

Three different types of analyses are carried out routinely; the most precise final solutions (daily) are produced about two weeks after observation by using the IGS final orbits; the rapid solutions (daily) are produced the next day after observation by using the IGS ultra rapid orbits; Quasi-real time solutions are obtained every 3 hours with a sliding window of six hours. The system is also capable of carrying out RTK-type analysis with 1 Hz data for selected baselines (less than 50 sites) whose ability was already demonstrated in the Tokachi Earthquake of September 25, 2003 (UT) (Figure 3).

The new system makes it possible to provide the information on crustal deformation in a timely fashion, and this is very important for responding to seismic or volcanic events.

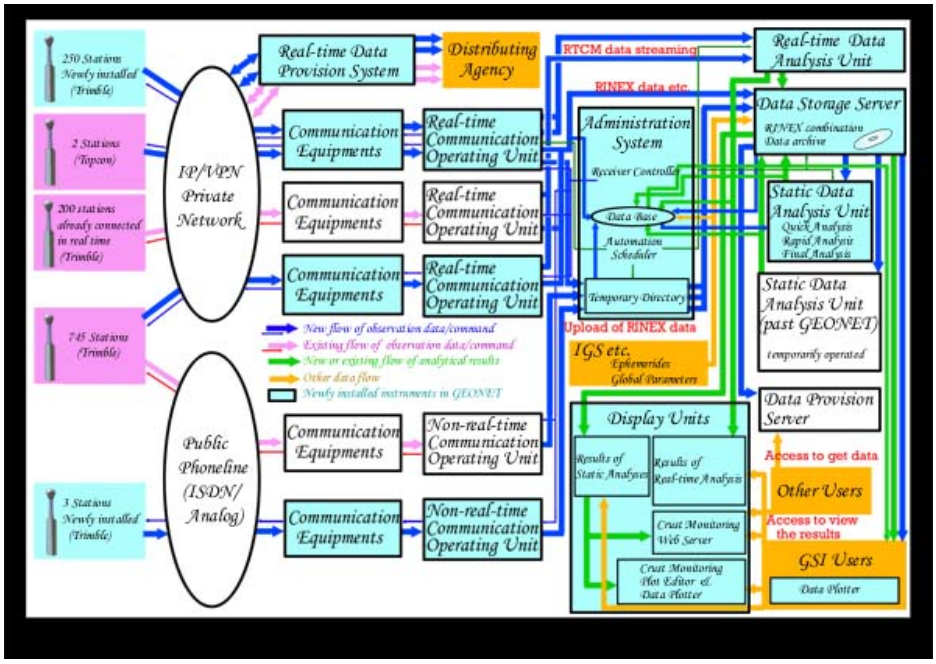

Figure 2. Data flow of new GEONET system.

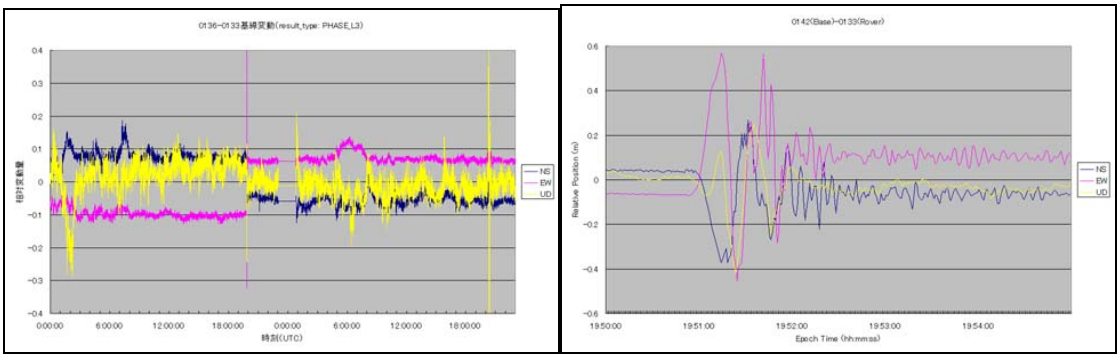

Figure 3 Time series of relative baseline components of 950133 (Biratori) referred to 950136 (Tomakomai) around the Tokachi Earthquake on Sep. 25, 2003. Time spans are 2 days (left) and 5 minutes (right).

Imaging the Source Region of the 2003 San Simeon Earthquake Within the Weak Franciscan Subduction Complex, Central California

Egill Hauksson, Seismological Laboratory, Pasadena, Caltech, CA 91125,
hauksson@gps.caltech.edu
David Oppenheimer and Thomas M. Brocher, USGS, MS 977, Menlo Park, CA 94025

Data collected from the 2003 Mw6.5 San Simeon earthquake sequence in central California and a 1986 seismic refraction experiment demonstrate that the weak Franciscan subduction complex suffered brittle failure in a region without significant velocity contrast across a slip plane. Relocated hypocenters suggest a spatial relationship between the seismicity and the Oceanic fault, although blind faulting on an unknown fault is an equally plausible alternative. The aftershock volume is sandwiched between the Nacimiento and Oceanic faults and is characterized by rocks of low compressional velocity (Vp) abutted to the east and west by rocks of higher Vp. This volume of presumably Franciscan rocks is interpreted as a highly compressed syncline embedded within the larger Santa Lucia anticline. High fluid saturation, implied by elevated Vp/Vs values, may control the limited depth distribution of the aftershocks within the hanging wall, between depths of 3 to 8 km. The paucity of aftershocks along the mainshock rupture surface may reflect either the absence of a damage zone or an almost complete stress drop within the low Vp or weak rock matrix surrounding the mainshock rupture.

Our 3D Vp and Vp/Vs models of the Santa Lucia Range image low crustal Vp and elevated Vp/Vs values down to depths of 15 km, which are typical of the Franciscan complex in central California. The 2003 San Simeon mainshock ruptured within the complex rather than along a lithological interface such as between gabbroic or granitic and Franciscan rocks as has been observed in other crustal mainshocks in central California. The lack of material contrast across the rupture plane suggests that the strain concentration may be related to the presence of abundant crustal fluids rather than an existing weak shear zone. The depth of faulting is limited to the upper 12 km of crust, with aftershock clusters of diameters of a few km, occurring both above and below the mainshock thrust plane. The aftershocks that occurred adjacent to the region of high mainshock slip are mostly confined to the hanging wall and do not image a well-defined fault zone. We attribute these strong clustering of off-fault aftershocks, in a limited depth range of 3 to 6 km, to the presence of moderately high Vp/Vs, which could be related to the presence of crustal fluids. In contrast, the deeper aftershocks may have occurred on existing mapped faults, such as the Nacimiento fault, and unmapped blind faults.

Supershear Rupture Transient Recorded During the 2002 Denali Fault Earthquake

Eric Dunham[1]
Ralph Archuleta[2]

[1]Physics Department, University of California, Santa Barbara
[2]Geological Sciences Department and Institute for Crustal Studies, University of California, Santa Barbara, edunham@umail.ucsb.edu

We construct a simple spontaneously propagating rupture model that reproduces the critical features of the near-fault ground motion recorded at Pump Station 10 of the Alyeska pipeline. This instrument was only 3 km off the fault. This velocity record has several distinguishing features. First, the fault parallel (FP) amplitude is approximately 1.5 times larger than the fault normal (FN). This is not typical of large strike-slip earthquakes. A single one-sided pulse (identify it as A) characterizes the fault parallel (FP) component. The pulse is narrow (approximately 3s pulse width) and roughly symmetric. The FN component contains two similarly narrow pulses, the first (identify it as B) concurrent with the FP. The second (identify it as C) arrives 2.6s later and is only slightly smaller in amplitude. Furthermore, about 6.5s after the initial pulse, a broad motion (identify it as D) begins on the FN component, comprising of motion toward and then away from the fault.

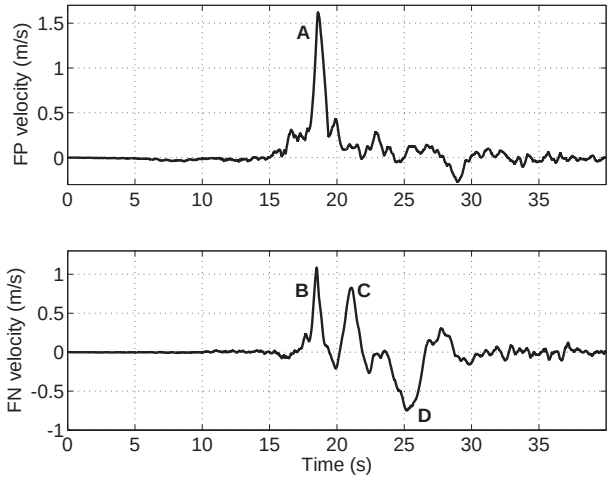

Several authors have suggested that the pulses A and B are due to supershear rupture (Ellsworth et al., 2004; Aagaard and Heaton, 2003). However, kinematic analyses which allow slip only once at the rupture front have failed to explain pulses C and D. We show that these pulses arise naturally in dynamic models that exhibit a transition from sub-Rayleigh to supershear rupture speeds; as such, it is a uniquely transient effect not present in steady-state solutions. A consideration of the dynamics of such a transition suggests that the breakdown in stress occurring behind the rupture front releases interface waves along the weakened fault that trail the faster-moving supershear front. These are essentially Rayleigh waves dispersed by friction, although, depending on the stability of the frictional sliding and rupture pulse width, these may be accompanied by a stress drop. These interface waves cause additional slip but carry almost all of their energy in FN motion (pulse C), hence their absence from the FP component.

For simplicity, and to demonstrate that a supershear transition is the only feature required to match the ground motion, we assume that all material and frictional properties are

uniform with depth. We construct a simple dynamic rupture model that exhibits a transition from sub-Rayleigh to supershear propagation and show that the ground motion explains several features recorded at PS10. We use a simple friction law that exhibits both slip-weakening and healing behaviors. The two-parameter law requires that the slip-weakening distance D and healing time T be specified at each point on the fault. We define the non-dimensionalized stress as $\theta = (\sigma_{xy} - \sigma_f) / (\sigma_y - \sigma_f)$ where σ_y and σ_f are the yield and sliding friction stress. The stress is governed by $\dot{\theta} = \frac{\theta \delta v}{D} + \frac{1-\theta}{T}$ once the fault begins to slip. Slip velocity is defined $\delta v = v_z(y = 0^+) - v_z(y = 0^-)$ and reverse slip is forbidden. This friction law is a modified form of one introduced by Nielsen & Carlson (2000) and provides a convenient way to introduce healing and generate rupture pulses. For $T \to \infty$ it reduces to an exponential slip-weakening law. Note that the slip-weakening distance for this model is twice that used in the standard linear slip-weakening model having the same fracture energy.

We artificially nucleate the rupture by slightly overstressing an asperity 61 km from the station, chosen to match the distance to the intersection of the Susitna Glacier and Denali faults. As several models have suggested (Harris et al., 1991; Harris and Day, 1993, Kase and Kuge, 1998; Magistrale and Day, 1999; Anderson et al, 2003), ruptures jump between faults almost exclusively when the initial rupture reaches the edge of the original fault. In our simulation the rupture begins bilaterally but we introduce a barrier 10 km to the west consistent with surface slip measurements (Eberhart-Phillips et al., 2003) that arrests propagation in that direction. We consider three faulting models; parameters are given in the table below. The fault depth is 10 km. The initial stress level θ_o is selected such that the rupture is sub-Rayleigh. To trigger the supershear transition, we increase the initial stress level to θ_a after the rupture has propagated approximately 25 km. No healing is used until the rupture encounters the high prestress region.

parameter		Model I	Model II	Model III
□	32.4GPa			
cs	3.4km/s			
cp	5.89km/s			
Grid spacing	125 m			
Time step	4.09 ms			
Distance to station	61 km			
Distance to asperity La		24.375 km	27.375 km	28.75 km
Fault width		10 km	10 km	5 km
□o (outside asperity)		0.45	0.45	0.70
□□ (within asperity)		0.70	0.77	0.87
□□□□		28.4 MPa	40.0 MPa	31.5 MPa
D	1.43m	1.43 m	2.01 m	1.58 m
T		∞	1.47 s	∞

In Model I upon reaching the region of increased prestress, the rupture smoothly accelerates from ~0.85 V_S to 1.6 V_S and continues at the supershear velocity as it passes the station. Even without any healing, the supershear rupture takes the form of a pulse, with the healing front trailing at the shear wave speed. The fault is locked until the Rayleigh arrival. This model gives too large of a pulse width to be consistent with the data, which requires a finite healing time on the order of one second. In Model II we introduce a healing front (T=1.47 s)

that follows at approximately the same speed as the supershear rupture front. A secondary slip pulse follows at the Rayleigh speed. This model produces results consistent with the data. An alternative method of producing a short pulse width is to have a length scale ~ 5 km; this is the essence of Model III where we constrained the fault width to be 5 km. It is not that we think the actual fault width is 5 km, but rather the region of stress heterogeneity responsible for the record at PS10 is of that order. At PS10 Model III produces results nearly identical to Model II.

Elastodynamic considerations suggest that the acceleration of ruptures to supershear velocities is accompanied by the release of Rayleigh waves from the stress breakdown zone. These waves generate a secondary slip pulse trailing the rupture front, but manifest almost entirely in ground motion normal (FN) to the fault in the near-source region. Acceleration from sub-Rayleigh to supershear velocities is accompanied by the release of a Rayleigh wave on the fault surface. This creates further slip and manifests itself primarily in FN ground motion, explaining late arriving FN pulses recorded at PS10. The multiple slip pulses that we observe in our dynamic models highlight the difficulty kinematic models may have when fitting supershear ruptures.

Differences in Earthquake Source and Strong Ground Motion Characteristics between Shallow and Buried Faulting

Paul Somerville, URS Corporation, Pasadena, CA, Paul_Somerville@URSCorp.com

Earthquake Rupture Models

During the past two decades, seismologists have gained much valuable information about the rupture process of earthquakes, including maps of subsurface slip on the fault plane, using strong motion recordings, teleseismic recordings, and geodetic data (Mendoza and Hartzell, 1988; Heaton, 1990). These rupture models describe not only the spatial distribution and orientation of slip, but also its temporal evolution. The slip models of shallow crustal earthquakes are characterized by strong spatial variation in slip on the fault surface, including asperities (which we may define as regions of large slip or slip velocity on the fault). There are also spatial variations in rupture velocity (the speed of propagation of the rupture front), and in slip velocity (the rate at which the fault slips at a point on the fault).

Slip models of enough crustal earthquakes have been derived over the past twenty years that we can now examine their systematic features, and use these systematic features to generate slip models for the prediction of strong ground motion (Irikura et al., 2003; Mai and Beroza, 2002; Somerville et al., 1999).

Shallow and Buried Faulting

Earthquakes typically nucleate near the bottom of the seismogenic rupture zone in the crust (Shimazaki, 1986). Large earthquakes usually break the surface, but small earthquakes usually do not (Wells and Coppersmith, 1994). Over one-half of the earthquakes in the magnitude range of 6.0 to 6.5 do not break the surface; this fraction decreases to about one-third for the magnitude range of 6.5 to 7, and about one-fifth of earthquakes in the magnitude range of 7.0 to 7.5 (Lettis et al., 1997). If it is assumed that all of the slip on a fault occurs during earthquakes, then larger earthquakes are characterized by relatively larger amounts of shallow slip than are smaller earthquakes. Further, on some faults, the breakage of strong asperities at depth on the fault in smaller earthquakes may be a precondition for the occurrence of a larger event with large shallow faulting. These differences in the depth distribution of slip are important, because it appears that the ground motions generated by earthquakes that do not have large shallow asperities are stronger than those of earthquakes that do.

Recent large earthquakes having large surface slip, including the 2002 Denali, 1999 Kocaeli, and 1999 Chi-Chi events, have surprisingly weak ground motions at short and intermediate periods. These new observations are consistent with our findings from previous earthquakes that the strong ground motions of earthquakes that have shallow asperities are weaker than the ground motions of events whose asperities are all deep (Kagawa et al., 2004; Somerville, 2003). The large differences in ground motion levels between these two categories of events are illustrated in Figure 1, which shows the response spectra of near-fault recordings of recent large earthquakes. The left panel shows recordings from four shallow earthquakes in the M_w range of 7.4 to 7.9, and the right panel shows recordings from two deep earthquakes of magnitude M_w 6.7 and 7.0. The response spectra of the deep earthquakes are much stronger than those of the larger

shallow earthquakes for periods less than 1.5 sec.

Comparing the distribution of slip with depth, averaged along strike, in the top part of Figure 2, this difference in ground motions between shallow and deep events seems paradoxical because the shallow events have much larger near-surface displacements. However, slip velocity is a much more important determinant of strong motion levels than fault slip alone (Dan and Sato, 1999). The effective slip velocity is defined by Ishii et al. (2000) as the slip velocity averaged over the time in which the slip grows from 10% to 70% of its final value, and represents the dynamic stress drop. As shown in Figure 3, the distribution of effective slip velocity with depth for shallow events is quite different from the distribution of slip with depth. The shallow events have large near-surface displacements, but they do not have correspondingly large slip velocities. The slip velocities of the deep events are larger than those of the shallow events, causing larger ground motion levels because slip velocity is an important determinant of strong motion levels. Averaged over 9 shallow events and 8 deep events, the slip velocity of shallow events is about 70% that of deep events. This is true both for the fault as a whole and for the asperities on the fault. We consider that this difference in slip velocity between shallow and deep events is an important aspect of earthquake source characterization for the simulation of strong ground motion.

References

Dan, K. and T. Sato (1999). A semi-empirical method for simulating strong ground motions based on variable-slip rupture models for large earthquakes, *Bull. Seism. Soc. Am.,* 89**,** 36-53.

Heaton, T. H. (1990). Evidence for and implications of self-healing pulses of slip in earthquake rupture, *Phys. Earth Planet. Interiors,* 64, 1-20.

Irikura, K., H. Miyake and L. Dalguer (2003). Characterization of source parameters of dynamic faulting for strong ground motion prediction. XXIII General Assembly of the International Union of Geodesy and Geophysics - IUGG2003, June 30 - July 11, 2003, Sapporo, Japan, SS04a/09P/D-032.

Irikura, K., H. Miyake, T. Iwata, K. Kamae, H. Kawabe, and L. A. Dalguer (2003). Recipe for predicting strong ground motion from future large earthquake, Annals of Disas. Prev. Res. Inst., Kyoto University, 46 (in press) (in Japanese with English abstract).

Ishii, T., T. Sato and Paul G. Somerville (2000). Identification of main rupture areas of heterogeneous fault models for strong motion estimation. *J. Struct. Constr. Eng., AIJ*, No. 527, 61-70.

Kagawa, T., K. Irikura and P. Somerville (2004). Differences in ground motion and fault rupture process between the surface and buried rupture earthquakes. *Earth, Planets and Space*, in press.

Lettis, W.R., D.L. Wells, and J.N. Baldwin (1997). Empirical observations regarding reverse earthquakes, blind thrust faults, and quaternary deformation: are blind thrust faults truly blind? *Bull. Seism. Soc. Am.,* 87, 1171-1198.

Mai, P. M. and G. C. Beroza (2002), A spatial random-field model to characterize complexity in earthquake slip, *J. Geophys. Res*., **107** (B11), 2308.

Mendoza, C. and S. Hartzell (1988). Aftershock patterns and mainshock faulting, *Bull. Seism. Soc. Am.,* **78**, 1438-1449.

Shimazaki, K. (1986). Small and large earthquakes: The effect of the thickness of the seismogenic layer and the free surface, Earthquake Source Mechanics, Am. Geophys. Union, Geophys. Monogr. 37, 209-216.

Somerville, P.G. (2003). Magnitude scaling of the near fault rupture directivity pulse. *Phys. Earth.Planetary.Int.*, 137, 201-212.

Somerville, P.G., K. Irikura, R. Graves, S. Sawada, D. Wald, N. Abrahamson, Y. Iwasaki, T. Kagawa, N. Smith and A. Kowada (1999). Characterizing earthquake slip models for the prediction of strong ground motion. *Seismological Research Letters*,70, 59-80.

Wells, D. L. and K. J. Coppersmith (1994). Analysis of empirical relationships among magnitude, rupture length, rupture area, and surface displacement. *Bull. Seism. Soc. Am.* **84**, 974- 1002.

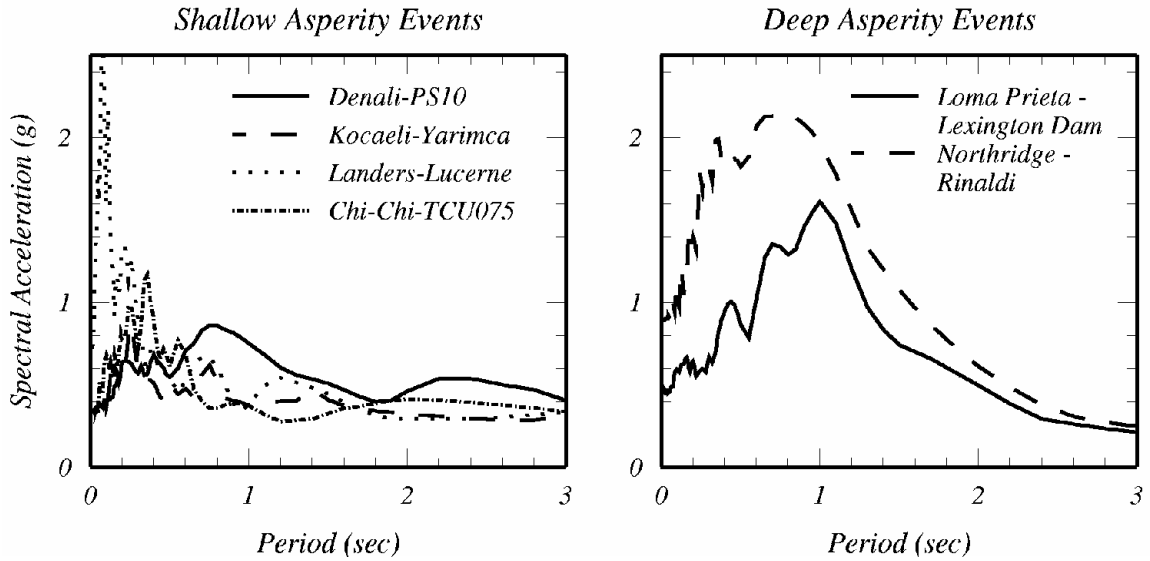

Figure 1. Near-fault response spectra of recent large earthquakes. Left: Four earthquakes, Mw 7.2 to 7.9, with shallow asperities and large surface faulting. Right: Two earthquakes, Mw 6.7 and 7.0, with deep asperities and no surface faulting.

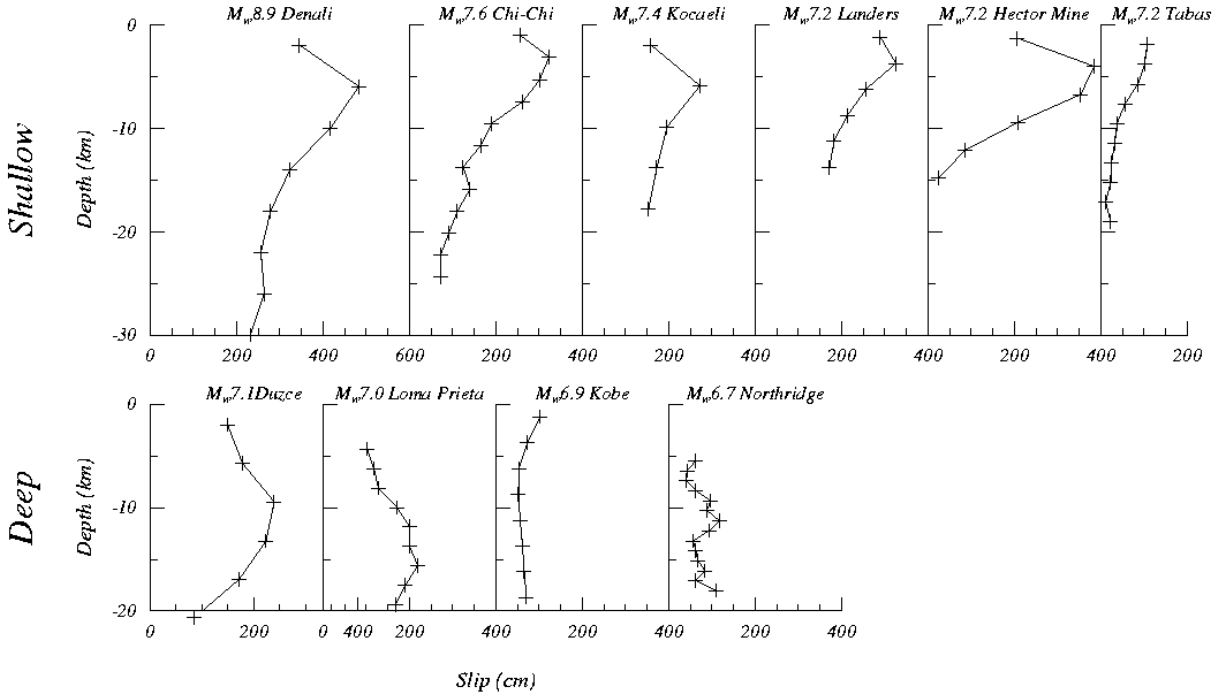

Figure 2. Distribution of slip for shallow (top) and deep (bottom) earthquakes.

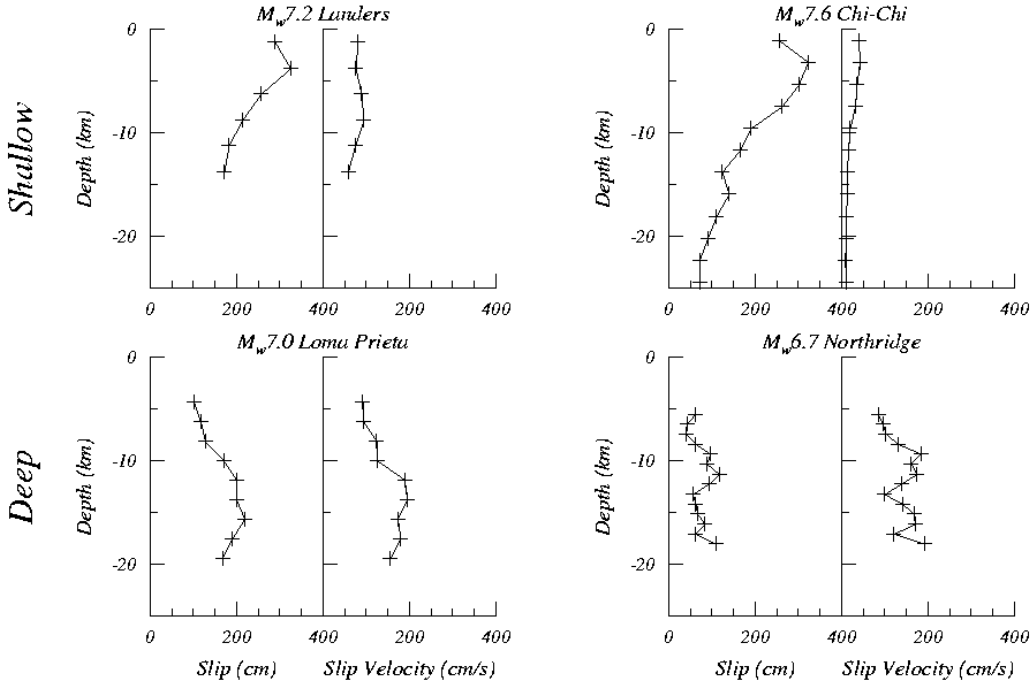

Figure 3. Distribution of slip (left) and slip velocity (right) for shallow (top) and deep (bottom) earthquakes. The left side shows two strike-slip earthquakes and the right side shows two thrust earthquakes.

Evidence of Non-linear Strong Ground Motion from Repeating Microearthquakes

Justin Rubinstein and Greg Beroza, Stanford University, Palo Alto, CA,
beroza@pangea.stanford.edu

We have identified time varying changes in seismic velocities following the 1984 Morgan Hill, 1989 Loma Prieta, and 1990 Chittenden earthquakes using repeating microearthquakes. Waveforms and source locations are nearly identical for all events within a repeating earthquake sequence, such that we can use moving window cross correlation to identify changes in arrival time well into the coda. The velocity changes we observe are always of the same sign (a co-seismic decrease) and are correlated with surface geology and, at least for the Loma Prieta earthquake where there is a shakemap available, the level of mainshock strong ground motion. The velocity decreases are ephemeral, and recover linearly with the logarithm of time following the earthquake that causes them. All of these observations are consistent with laboratory studies of the nonlinear response of rock samples to oscillatory strains in excess of about one part in a million at ambient conditions. Thus, we believe that with the velocity decreases we observe are the lingering effects of nonlinearity (damage) in the shallow crust during strong ground motion. Monitoring of repeating earthquake sequences, when available, may lead to new insights into the conditions under which strong ground motion enters the nonlinear regime.

Slow earthquake families on the subducting Philippine Sea plate in southwest Japan: Non-volcanic tremor, slow slip and very low-frequency earthquake

Kazushige Obara, National Research Institute for Earth Science and Disaster Prevention, Japan, obara@bosai.go.jp

The Nankai trough subduction zone in southwest Japan is characterized by "slow earthquakes". Around the downdip side of the seismogenic zone on the subducting Philippine Sea plate, non-volcanic tremors are distributed in a narrow belt along the strike of the plate with a length of 600km from Tokai to Kyushu in southwest Japan. The tremor signal has a frequency between 1.5 and 5 Hz, and usually lasts from hours to weeks. In some areas of the belt-like distribution, short-term slow slips with durations of about 1 week occur accompanied by active tremors. In the western part of Shikoku Island, the coupling phenomena of the slow slip and major tremor activity were clearly observed with a recurrence interval of 6 months during 2001 and 2002. In this two-year time span, the source of the tremors and slow slip migrated along the strike of the subducting plate. The episodic activity of tremor and slow slip is very similar to the phenomena detected in the Cascadia subduction zone. Around the Bungo Channel, between the Kyushu and Shikoku Islands, an intermediate long-term slow slip event with a duration of about three months occurred in late 2003. At the same time, the tremor activity continued intermittently in the same area. The tremor sequence is the longest activity since monitoring of these tremors was started in 2000. In this area, 7 years ago, a similar long-term slow slip event was detected by GPS. In the Tokai area, central Japan, a slow slip event has continued for longer than a few years. The tremors beside the Tokai slow slip area includes some episodic activity; however there are no short-term slow slip events like have been detected in Cascadia or in the western part of Shikoku.

On the other hand, in shallower segments of the seismogenic zone, anomalous seismic activity has been detected. The waveform of the earthquake is characterized by a band-limited low-frequency content between 10 and 20 seconds in length. We call the earthquake a "very low-frequency (VLF) earthquake." Seismograms were generated with a bandpass filter of 10 to 100 seconds operated on the output of the high-sensitivity accelerometer (tiltmeter) installed in every NIED Hi-net station for detection and further analysis. The waveform of the VLF earthquake is similar to that of teleseismic events, however the spatial pattern of the amplitude and the apparent velocity of the VLF earthquake are quite different from those of teleseismic events. Because waveforms of the VLF earthquake are quite similar in neighboring stations, epicenters are estimated by using a cross-correlation analysis. The Hi-net stations in southwest Japan are divided into groups with a diameter of about 100km. The cross-correlation is calculated for every pair of stations in each group in order to measure the lag time which gives the highest cross-correlation coefficient. Then, the set of lag times obtained for each group are used to estimate the propagation direction and the apparent velocity. Finally, the epicenter of the VLF earthquake is estimated by focusing the back projection of the ray propagation for each group. In the year 2003, there were two active clusters of the VLF event near the Nankai trough; off Cape Muroto and the Hyuga-nada region. The VLF seismic activity usually lasts for a month in each cluster. Both activities were located on the seaward updip portion of the seismogenic zone on the subducting Philippine Sea plate. Just after the occurrence of the 2003 Tokachi Earthquake in northeast Japan on September 26, 2003, the VLF seismic activity in the eastern part of the Hyuga-nada region became very active and continued for a month. Considering the reverse fault type mechanism and shallow depth estimated by the centroid moment tensor (CMT) analysis, the VLF earthquakes might occur in the accretionary prism or on the decollement.

Moreover, both active clusters correspond to the extension of the chain-like sea mounts on the ocean floor of the Philippine Sea. Therefore, the occurrence of the VLF earthquake might be related to the existence of the subducting sea mount.

At present, there is no clear relationship between the episodic tremor and slow slip and the VLF earthquake activity in their time histories. However, both seismic phenomena are located on transition zones between the locked zone and decoupled aseismic zones on the subducting plate boundary. Therefore, these low-frequency families must be representing the subduction process of the young oceanic plate.

Observations of deep, non-volcanic tremor in Cascadia

Steve Malone, Wendy McCausland, and Dan Johnson, University of Washington, Seattle, WA, wendy@ess.washington.edu

Episodic Tremor and Slip Events (ETS) have been observed in Cascadia by a group from the Pacific Geoscience Centre (Geological Survey of Canada) and the Pacific Northwest Seismograph Network (University of Washington). This tremor is similar to and assumed to be the same phenomenon as reported by Obara (2002) in southern Japan. It has frequency content between 1-6Hz, lasts anywhere from tens of seconds to hours, is made up primarily of S-waves and varies in amplitude over periods of seconds to tens of seconds. Concentrated bursts of tremor lasting ten days or more are associated with geodetically determined slip on the deep part of the subduction zone interface. Four relatively independent zones of concentrated tremor have been identified, northern Vancouver Island, northern Puget Sound-southern Vancouver Island, southern Puget Sound and northern California. The PGC team has identified repeating episodes of ETS events at 14 month intervals for the past ten years for the two northern zones. Reviews of PNSN and northern California data have just begun and thus a long-term pattern for these two zones has yet to be determined. An area in central Puget Sound is overlapped by two different tremor zones and undergoes tremor activity during both sets of slip events as well as short periods of tremor not associated with geodetically detectable slip (Fig. 1).

During the spring and summer of 2004 three small aperture arrays were operated in the northern Puget Sound area to capture the latest ETS. Preliminary analysis of two arrays indicates very high correlation of waveforms across each array with the capability to resolve back-azimuth and slowness to better than 10 degrees and 0.025 sec/km respectively for strong tremor periods (Fig 2). Preliminary analysis indicates that SH waves dominate and that tremor sources can change locations over periods of a few minutes. We are experimenting with several different array processing techniques to determine the most efficient and effective technique for processing all of the array data. By tracking the changes simultaneously from the three arrays we hope to be able to follow the progression of tremor locations over a whole tremor episode.

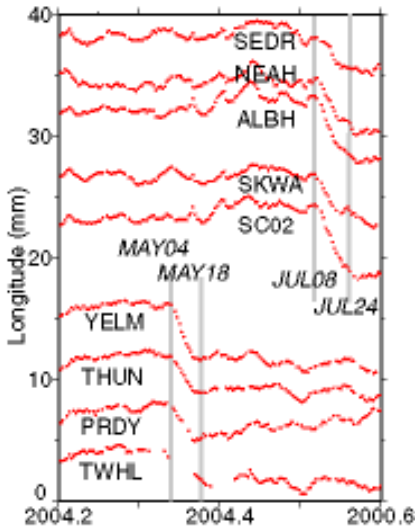

Figure 1. GPS motions for stations ordered north to south. Note south event (May 4-18) and north event (July 8-24).

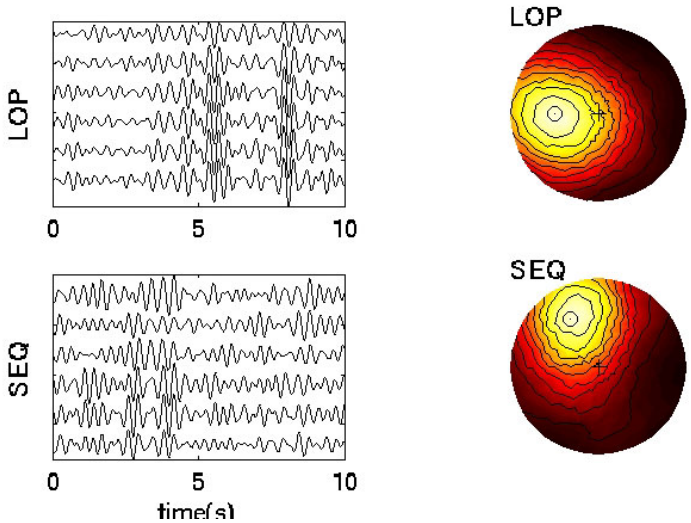

Figure 2. Sample trace data from array, LOP and SEQ and polar plot of azimuth and slowness of beam-formed stack. Source is west of LOP and NNW of SEQ.

Repeating short- and long-term slow slip events with deep tremor activity around Bungo channel region, southwest Japan

Hitoshi Hirose and Kazushige Obara, National Research Institute for Earth Science and Disaster Prevention (NIED), Japan, hirose@bosai.go.jp

Non-volcanic deep low-frequency tremors are observed at the Nankai trough subduction zone, southwest Japan (Obara, 2002). This observation is thought to be a manifestation of the dehydration processes in the subducted slab. This plays an important role in exploring not only the material circulation associated with plate subduction, but also has an effect on the process of generating large shallow earthquakes.

Recently, Obara et al. (2004) reported that a crustal tilt change, accompanied by deep tremor activity, is observed by high sensitivity accelerometers (tiltmeters) equipped with NIED Hi-net (National Research Institute for Earth Science and Disaster Prevention, Japan; High sensitivity seismograph network). This deformation can be interpreted as a slow slip event (SSE) on the plate interface at depth. In western Shikoku, this activity repeats every six months. Each episode has a duration of about a week and a corresponding moment magnitude of 6.0. The estimated depth is 30–40 kilometers, showing that this activity may occur at the transition zone of interplate coupling. We call this phenomenon 'short-term SSE.'

We have another SSE event, the 'long-term SSE,' which occurred beneath the Bungo channel, adjacent to western Shikoku, where short-term SSE with tremors repeatedly occurs. In 1997, an SSE was detected by GSI's (Geographical Survey Institute, Japan) nationwide GPS network (e.g., Hirose et al., 1999). This event lasted for about one year. Similar crustal deformation reappeared in 2003 (Ozawa et al., 2004). This deformation was observed by both GPS and tiltmeters. The tilt change began in late August and lasted for about three months. The maximum tilt change was about 0.6 μrad. The surface displacement also showed a large and relatively fast change which began in late August, though the very small, relatively slow change in displacement seemed to start in early 2003. Both the observed GPS time series and the surface displacement field for both events in 1997 and 2003 are quite similar. This evidence suggests that the same source area sliped in these two episodes.

Preceding the acceleration of crustal deformation due to the long-term SSE in late August 2003, a short-term episode took place in the Bungo channel west of the Shikoku region. This implies that the short-term SSE works as a precursory slip event, leading to the main phase of the long-term SSE. Since this episode, we have observed a change in periodicity and size of the short-term episodes, i.e., three other episodes that occurred from November 2003 to April 2004, and they may have a smaller source area than the 2001 and 2002 episodes. This suggests that the long-term SSE triggers nearby short-term SSEs and hastens these occurrences.

Some of these episodes have nearly the same surface deformation pattern. This shows the existence of ‘slow slip patches’ on the plate interface, where the episodic slow slip is the characteristic slip behavior and the size of the event is almost constant during several recurrence cycles.

Low-frequency tremor and slow slip around the probable source region of the Tokai Earthquake: A new indicator for the Tokai Earthquake prediction provided by unified seismic networks in Japan

Noriko Kamaya, Seismological and Volcanological Department, JMA, Akio Katsumata, Meteorological College, JMA, akatsuma@mc-jma.ac.jp, and Yuzo Ishigaki (Seismological and Volcanological Department, JMA

Since Oct. 1997, short-period seismic records observed at most stations in Japan have been transmitted to the Japan Meteorological Agency (JMA). The JMA has processed those records to make a unified seismic catalog in Japan. The short-period instruments include those installed by the National Research Institute for Earth Science and Disaster Prevention (NIED), universities, the JMA, other national institutes and local governments. This integrated processing lowered the detectable magnitude of earthquakes. Moreover, deployment of the Hi-net which is a dense network of highly-sensitive short-period instruments installed by the NIED, improved detection ability remarkably. Hi-net data has been included to produce the seismic catalog since Oct. 2000.

The enhanced detection ability revealed the occurrence of low-frequency events in Japan. The JMA has distinguished low-frequency earthquakes in the seismic catalog since 1999. Occurrence of low-frequency events around the Moho discontinuity in the areas away from volcanoes became recognized based on the seismic catalog [Nishide et al., 2000]. The most notable activity is a belt distribution of deep low-frequency continuous tremors along the strike of the subducting Philippine Sea plate in southwestern Japan. Source depths of these tremors were estimated at 25-35 km. The source is assumed to be around the boundary region between oceanic and inland crusts close to the mantle wedge.

The east end of the belt tremor distribution is adjacent to the probable source region of the Tokai Earthquake. A slow-slip event has been continuous west of the source region of the Tokai Earthquake since 2000. Synchronous activation of the tremor and slow-slip speed was observed in 2003. This indicates some relationship between slow-slip and tremor activity. We expect that the tremor activity could be a new valuable indicator for the Tokai Earthquake prediction. But the relationships between large earthquakes or earthquake swarms and the occurrence of the tremor are yet to be determined clearly.

The long duration of the tremor is considered to be related to some kind of fluid or ductile material. We assume that water would be related to the tremor. The restricted depth range of tremor activity is related to a limited pressure and temperature condition. Based on the results of high pressure and temperature experiments on water-saturated oceanic basalt and peridotite, the water released by the dehydration of chlorite (to form clinopyroxene in the basalt of the descending Philippine Sea Plate) could be a possible trigger. The descending oceanic crust begins contact with the mantle wedge under the northern rim of the belt. Because the temperature would be low enough for mantle peridotite in the mantle wedge to absorb ascending water by forming hydrous minerals, the northern border of the belt distribution is possibly rimmed by the mantle wedge.

Research in Earthquake Physics, Forecasting, and Simulation-Based Probabilistic Hazard Assessment at the University of California, Davis

Donald L Turcotte, University of California, Davis, turcotte@geology.ucdavis.edu

At the University of California, Davis, we are pursuing multiple approaches in earthquake research. Most of our methods grow out of statistical physics approaches to understanding the dynamics of driven threshold systems such as earthquake fault systems. Besides earthquakes, other examples of driven threshold systems include neural networks, the forest fire model, the SOC sandpile model, driven foams, and magnetic de-pinning transitions.

In the area of earthquake forecasting, we have pioneered a new approach, Pattern Informatics, which uses observed seismicity changes to construct a state vector characterizing the time- and space-dependent evolution of the fault system in seismically active areas such as southern California. These state vectors are then used to compute a probability index forecasting future activity of large events, by computing the change in state over a period of time preceding the forecast interval. Probability change is then found by squaring the state vector difference, then subtracting off the average background rate. We have evaluated the accuracy of our forecasts using statistical hypothesis testing, and found that our methods have high forecast skill. Our forecast for the period 2000-2010 can be found at http://quakesim.jpl.nasa.gov/scorecard.html .

In the area of simulation-based seismic hazard assessment, we are focusing on new, topologically realistic system-level approaches to the modeling of earthquake fault systems using a model we developed, Virtual California. Virtual California is a “backslip model”, meaning that the long term rate of slip on each fault segment in the model is matched to the observed rate. The faults in the model interact by means of quasistatic elasticity, and frictional dynamics are based on laboratory friction experiments. Constraints for the input parameters for these models originate from field data, and typically include realistic fault system topologies, realistic long term slip rates, and realistic frictional parameters. Outputs from the simulations include synthetic earthquake sequences and space-time patterns, together with associated surface deformation and strain patterns that are similar to those seen in nature. Our simulations can be used to compute, or “measure”, empirical statistical distributions (probability density functions: PDFs) that characterize the activity. Examples include PDFs for recurrence intervals on selected faults. These PDFs can be used to construct probabilistic seismic forecasts for selected faults or groups of faults. The major difference between the simulation-based method and current statistical approaches lies in the way in which inter-event times and probabilities for joint failure of multiple segments are computed. In our simulation-based approach, these times and probabilities come from the modeling of fault interactions and laboratory-based friction laws.

In this talk, I will summarize these complementary approaches, as well as how the results of our research might be used in practice.

New System of Information about the Tokai Earthquake based on Pre-slip Models

Noriko Kamaya and Hidemi Ito, Seismological and Volcanological Department, Japan Meteorological Agency, kamaya@met.kishou.go.jp

A great earthquake is expected to occur along the Suruga Trough where the Philippine Sea plate subducts beneath the Eurasian plate. The earthquake has been named the Tokai Earthquake even prior to its occurrence. The Japanese government has taken countermeasures against the earthquake, including predictions since 1978. The Japan Meteorological Agency (JMA) is responsible for issuing predictions on the earthquake when precursory changes appear in data obtained through a dense observation network in the Tokai area. The Tokai Earthquake is the only one for which prediction is included in the national disaster prevention efforts.

The countermeasures for the Tokai Earthquake were initially designed by assuming the appearance of a clear precursory crustal movement, as was observed just before the Tonankai earthquake (M7.9) in a region contiguous to the Tokai area in 1944. They call for issuance of warnings and tight restrictions to be imposed on the transportation system and daily activities of the residents. Recent developments of seismology have shown that such a clear precursor does not always occur, and thus it is necessary to minimize social and economical risks of a false alarm.

The JMA has examined possible scenarios leading to the Tokai earthquake on the basis of the recent development of pre-slip models, and provided a warning system of three levels corresponding to those of the crustal anomaly. At the lowest level, disaster prevention organizations and the general public take a wait-and-see policy. At the advisory level, only the former take preparatory action. At the warning level, both take countermeasures against the earthquake. In case the crustal anomaly is too small to detect, or the anomaly is smaller than that estimated by the models, it will be impossible to issue the information appropriately. The public are advised to prepare for the worst case scenario in which the earthquake could occur suddenly and without any warnings. In this scheme, as long as the observed anomaly is restricted to seismicity, only the lowest level warning would be issued.

We first sketch recent developments of the 3D simulation of the plate subduction in the Tokai area. Then we present how the crustal anomaly is used to determine the level of warning.

Search for Precursor and Coseismic Signals: EM data, GPS TEC, Thermal Mapping of California Faults

E. Calais, Purdue University, West Lafayette, IN, ecalais@purdue.edu
T. Bleier, Quakefinder, Palo Alto, CA

Electromagnetic emissions related to earthquakes have been reported in various tectonic settings, with, in some cases, simultaneous ionospheric disturbances, but several of these studies raise suspicion as far as a proven causative relationship between the earthquake and the electromagnetic and ionospheric signals. Since most of these observations were made with equipment that was not specifically designed for the purpose of recording earthquake-related signals, the observations are discontinuous in time, often do not cover the most appropriate frequency bands, and are not spatially redundant. A critical test of a relationship between earthquakes and electromagnetic emissions consequently requires the use of specifically designed equipment, installed in key areas with respect to the expected seismicity distribution, with a high density and as much redundancy as financially and logistically possible.

Here we report preliminary results of a study aimed at combining electromagnetic (EM) data and ionospheric electron content (TEC) measurements from Global Positioning System (GPS) data to search for earthquake precursors and coseismic signals in California. This project is based on data from existing sensors (SCIGN GPS stations, CLEO and CalMagNet EM stations, and satellite data) and from twelve additional Extremely Low Frequency (ELF) sensors that are being installed in areas mapped with a highly probable near-term M>5 seismic activity.

QuakeSim: Simulation and analysis tools for creating a solid Earth science framework for understanding and studying active tectonic and earthquake processes

Margaret Glasscoe and Andrea Donnellan, Jet Propulsion Laboratory, California Institute of Technology, Pasadena, CA, Margaret.T.Glasscoe@jpl.nasa.gov

We are developing the QuakeSim problem solving environment for scientists in the seismological, crustal deformation, and tectonics communities to provide simulation and analysis tools to study the physics of earthquakes. This problem solving environment utilizes state-of-the-art modeling, data manipulation, and pattern recognition technologies and is being developed with an interoperability framework that allows integration of heterogeneous data sources and the variety of application programs, tools, and simulation packages making up the environment.

We are developing clearly defined accessible data formats and code protocols as inputs to the simulations. These codes are adapted to high-performance computers because the solid Earth system is extremely complex and nonlinear, resulting in computationally intensive problems with millions of unknowns.

QuakeSim includes three high-end computing simulation tools: GeoFEST, PARK and Virtual California and a number of software applications that can be used individually or can interact with other applications in the environment (including inversion programs, statistical analysis and pattern recognition applications, and visualization tools), as well as a fault database with California faults. These are all packaged in a prototype web services portal that links these diverse applications on distributed computers.

QuakeSim provides a critical framework for studying active tectonics and earthquake processes. Without these tools, it will be impossible to construct the more complex models and simulations necessary to develop hazard assessment systems critical for reducing future losses from major earthquakes.

Conventionally detected crustal deformation in Tokai region

Masaru Kaidzu, Geographical Survey Institute, Japan, kaizu@gsi.go.jp

Slow slip events presently observed in the Tokai region are a unique phenomenon in the past 30 years. There are discussions that slow slip repeatedly occurred in this region. We examined results of conventional surveys, especially leveling surveys. The time-space chart of vertical displacement shows that the area of subsidence tended to spread toward the west in the period 1977- 1983 and shrank in the period 2000-2004. We can observe fluctuations over a time scale of only about three years. The observed amplitude, however, is often much smaller than that of the present event.

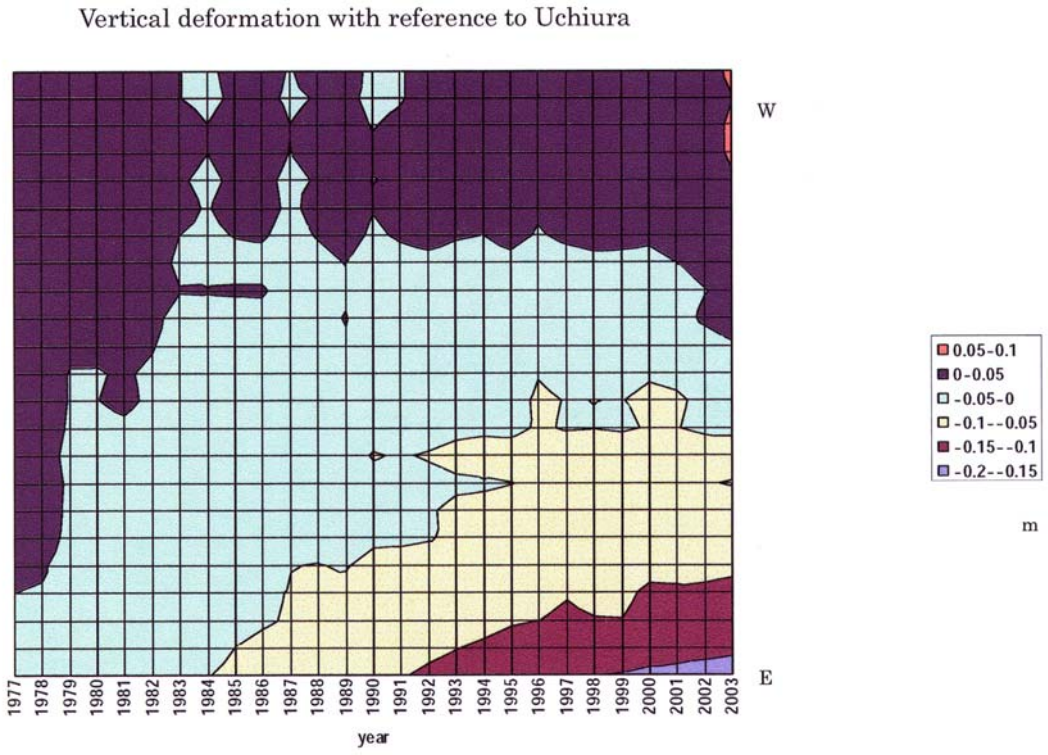

Foreshock Sequences and Short-Term Earthquake Predictability on East Pacific Rise Transform Faults

Jeffrey J. McGuire and Margaret S. Boettcher, Woods Hole Oceanographic Institution, Woods Hole, MA

Thomas H. Jordan, University of Southern California, Los Angeles, CA, tjordan@usc.edu

Mid-ocean ridge transform faults (RTFs) have many properties that are distinct from continental transform faults: most plate motion is accommodated aseismically, many large earthquakes are slow events enriched in low-frequency radiation, and the seismicity shows depleted aftershock sequences and high foreshock activity. Because of the high ratio of foreshocks to aftershocks, RTF earthquakes cannot be explained by standard point-process models of seismic triggering, in which there is no fundamental distinction between foreshocks, mainshocks, and aftershocks. A retrospective analysis of the post-1996 NOAA-PMEL hydroacoustic seismicity catalogs demonstrates that foreshock sequences on East Pacific Rise (EPR) transform faults can be used to achieve statistically significant short-term prediction of large earthquakes (magnitude $\geq$ 5.4) with good spatial (15-km) and temporal (1-hr) resolution. The predictability of EPR transform earthquakes is consistent with a model in which slow slip transients trigger earthquakes, enrich their low-frequency radiation, and accommodate much of the subseismic plate motion.

Effects of Fluid Pressure Changes on Borehole Strainmeter Data: Studies in Preparation for the Earthscope Plate Boundary Observatory

Evelyn Roeloffs, U.S. Geological Survey, Vancouver, WA, evelynr@usgs.gov

The Plate Boundary Observatory (PBO) component of the Earthscope initiative, funded by the United States National Science Foundation, will deploy approximately 140 borehole strainmeters in tectonically active parts of the western United States. It is recognized that subsurface fluid pressure changes influence borehole strainmeter data, and therefore PBO boreholes will also be instrumented with continuous fluid pressure sensors. The hope is that the fluid pressure data will be able to be used to correct the strainmeter data for variations due to fluid pressure changes. This possibility is evaluated by analyzing the existing records of pore pressure and strain from the six California sites where these measurements are now made in close proximity. Similar datasets exist in Japan and could also be evaluated in these ways.

The "coupling effect" is one of the ways in which fluid pressure changes influence borehole strainmeter data. In settings where large fluid pressure changes take place due to infiltration of precipitation, strainmeter output can be expected to contain signals produced by these pressure changes. Coupling introduces ambiguity with respect to distinguishing tectonically-induced strain changes from fluid pressure changes. Strain changes that may be due to the coupling effect are observed in California at several dilatometer and three-component borehole strainmeter sites.

The "drainage effect" is another way that fluid flow can affect borehole strainmeter data. When tectonic strain induces fluid pressure changes (e.g., fluid pressure increases in regions subjected to coseismic static contractional strain), these fluid pressure changes will recover by flow to the water table on a time scale depending on the depth and vertical hydraulic diffusivity. As this flow takes place, it will apply stress to the strainmeter (e.g., relative tensional stress as fluid pressure decreases), leading to apparent recovery, or partial recovery, of the coseismic static strain step. This apparent recovery has the potential to mask the time-dependent effects of horizontal pore fluid flow or viscous relaxation that might be related to tectonic post-earthquake processes.

Effects of drainage on strainmeters operating in California have been evaluated by looking at the frequency dependence of atmospheric pressure response and any possible recovery occurring after coseismic steps. Analysis to date shows that two dilatometers are probably affected by drainage at periods longer than 10 and 20 days, respectively.

The results of this study will be used to help plan the PBO strainmeter installations. Aquifer tests will help determine the degree of drainage that is likely to be encountered, by placing constraints on the hydraulic diffusivity of the rock in which each instrument will be installed. Hydrologic parameters obtained from aquifer tests will also be useful in estimating fluid pressure changes at the precise strainmeter location, given fluid pressure measurements made several tens of meters above the strainmeter. The intention is to avoid placing strainmeters in settings where drainage is expected to be significant, and to design the best possible way of monitoring fluid pressure in each borehole.

In situ Measurement of Rock Viscosities by Sakata-type Three-component Strainmeters

Shoji Sakata, National Research Institute for Earth Science and Disaster Prevention,
sakata@bosai.go.jp

We have been carrying out continuous observations with Sakata-type three-component strainmeters for more than 22 years in Yasato and more than 17 years in Kofu. Observational records show that three area-time curves of any instrument are very similar, and each curve is composed of a time-decaying component and a linearly-changing component with time. This time dependent deformation is rock creep. The time-decaying component of the observed curve is the transient creep and the linearly-changing component with time is the steady state creep. In this presentation, we discuss steady state creep, which is derived from knowing the character of Maxwell material.

To analyze the steady state creep, we introduced an equivalent tensile stress distributed on the borehole wall. Before drilling a borehole, the rock mass had been subject to a nearly hydrostatic compression, whose absolute value is proportional to the weight of the rock column with the unit area. After drilling, compressive stress on the borehole wall vanishes. This is equivalent to superposition of a tensile stress $\rho_m gH$ on the borehole wall. It is supposed that a borehole wall has been pulled toward the center by this equivalent stress. We derived an equation to relate the gradients of steady state creep curves to viscosities of surrounding rocks, which are supposed to be Maxwell materials.

We obtained viscosities of (2-3)×10E19 Pa.s from the data of Yasato No1, and No2 instruments installed in two 160m boreholes in granite and 1×10E20 Pa.s from Kofu in a 140m depth borehole in granite. Since *in situ* measurement is carried out in natural conditions the reliability is estimated to be high compared to the laboratory method, which is inevitably affected by different conditions. One disadvantage of this method is that a period of at least ten years is necessary before the transient creep component decays enough to make the stationary creep component distinct.

So far we have neglected the long-term deformation of tectonic origin. Since the deformation by creep seems far larger than that by tectonic stresses, it is particularly difficult to distinguish differences between the three gradients of creep curves. This does not contradict the fact that short-period fluctuations or changes of tectonic stresses are detected with high resolution by this instrument.

Viscosity plays an important role in stress accumulation relative to earthquake occurrence. When a Maxwell material is subject to a strain increasing with constant rate, which represents the tectonic motion, the stress-time curve is expressed as; $\tau(t) = G\gamma_0 \exp(-t/t_m) + V\eta(1-\exp(-t/t_m))$,

where G : rigidity, γ_0 : initial strain, $t_m(=\eta/G)$: Maxwell relaxation time , V : rate of strain increase, η : viscosity. Qualitatively, elasticity is dominant along the beginning of the curve where stress increase is proportional to strain (time). On the other hand, viscosity becomes dominant later, when an increase in strain does not necessarily translate to an increase in stress.

If we combine this stress-time curve with rock strength, useful assumptions about occurrence intervals of earthquakes could be obtained. For a more precise solution, we need to determine the viscosity values of rocks located in the zones where earthquakes occur. To accomplish this, we need a borehole strainmeter which can withstand higher temperatures. A Sakata-Gubin laser strainmeter could be a candidate for that purpose.

Constraining the rupture process of the September 25, 2003 Tokachi-Oki earthquake using 1-Hz GPS data

Shin'ichi Miyazaki, Earthquake Research Institute, University of Tokyo, and Department of Geophysics, Stanford University

Kristine M. Larson and Kyuhong Choi, Department of Aerospace Engineering Sciences, University of Colorado, Kristine.Larson@colorado.edu

Kazuhito Hikima and Kazuki Koketsu, Earthquake Research Institute, University of Tokyo

Paul Bodin, Center for Earthquake Research and Information, University of Memphis

Jennifer Haase and Gordon Emore, Department of Earth and Atmospheric Sciences, Purdue University

Atsushi Yamagiwa, Geographical Survey Institute of Japan

The 25 September 2003 Tokachi-Oki earthquake generated large permanent surface displacements in Hokkaido and dynamic displacements exceeding one meter. Although not designed for seismic applications, 1-Hz GPS recordings of this earthquake were analyzed to recover both dynamic and static seismic displacements. Records from 37 sites on the Japanese islands of Hokkaido and Honshu were used to estimate the time history of fault-slip during the rupture. It was found to propagate downdip in the subduction zone with significant moment release ~ 80 km northwest of the hypocenter. The region of largest slip agrees in general with traditional seismic studies, indicating that 1-Hz GPS can be used for finite fault studies. Our slip model is consistent with afterslip/aftershock distribution.

Hydrological changes induced by the 2003 Tokachi-oki Earthquake, Japan

Norio Matsumoto(1), Fujio Akita(2), Tsutomu Sato(1), Naoji Koizumi(1), Yuuichi Kitagawa(1), and Makoto Takahashi(1)

(1) Geological Survey of Japan, National Institute of Advanced Industrial Science and Technology (AIST), Tsukuba, Japan
(2) Geological Survey of Hokkaido, Sapporo, Japan

Many hydrological changes were caused in and around Hokkaido, Japan by the 2003 Tokachi-oki earthquake (M8.0). We will mainly discuss the coseismic hydrological changes and compare them to coseismic volumetric strain changes calculated from the fault model in this presentation.

In Hokkaido, coseismic steps in the groundwater level or discharge rate at thirty-two wells and at an undersea coal mine were detected (Fig.1). Most of the increases and decreases in the groundwater levels or discharge rates can be explained as a poroelastic response to the earthquake-induced volumetric strain changes inferred from a fault model determined by dense static GPS observation (Fig.1) (Geographical Survey Institute, 2003). At five of the wells, the relationship between the groundwater-level changes and volumetric strain changes is consistent with observations from the past four large earthquakes ($M > 7.5$) in and around Hokkaido in 1993-1994. At three of the five wells, strain sensitivities of the groundwater levels determined by the relationship between the coseismic groundwater-level changes and strain changes are consistent with those estimated from analysis of tidal changes in the groundwater levels (Akita and Matsumoto, 2004). The oscillations in the groundwater level associated with the tsunami caused by the 2003 Tokachi-oki earthquake were also observed in several wells.

Coseismic groundwater level steps associated with the 2003 Tokachi-oki earthquake were also detected at ten of the forty-two observation wells in Honshu, Japan, some of which are located about 1,000 km away from the epicenter (Fig.2) (Sato et al., 2004). Seven of the ten increases or decreases in the groundwater levels or discharge rates can be explained as a poroelastic response to the earthquake-induced volumetric strain changes (Fig.2). At five of the seven changes, strain sensitivities of the groundwater levels estimated from the coseismic steps are almost consistent with those from tidal changes in the groundwater levels.

References

Akita and Matsumoto (2004) Hydrological responses induced by the Tokachi-oki earthquake in 2003 at hot spring wells in Hokkaido, Japan, Geophys. Res. Lett., 31, in press.

Geographical Survey Institute (2003), http://www.gsi.go.jp/WNEW/PRESS-RELEASE/2003/0926-2.htm (in Japanese).

Sato et al. (2004) Changes in groundwater level associated with the 2003 Tokachi-oki earthquake, Earth Planets Space, 56, 395-400.

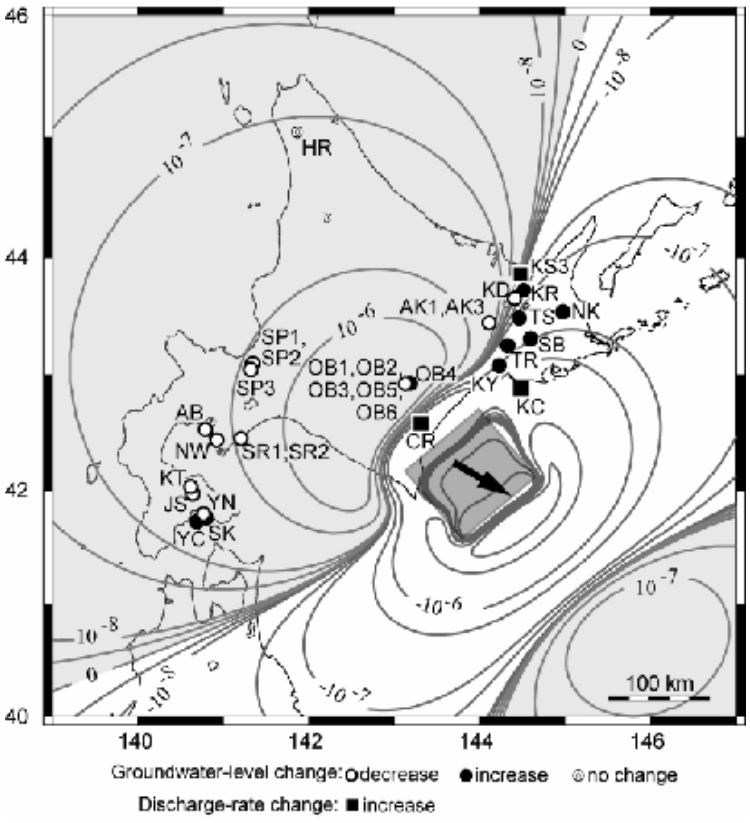

Fig.1

Location of observation sites in Hokkaido, Japan. A hatched square indicates the fault model of the 2003 Tokachi-oki earthquake by the Geographical Survey Institute (2003). Contours denote the coseismic volumetric strain changes at the depth of 500m calculated from the fault model. Positive and negative values denote dilatation and contraction, respectively. Solid circles and squares denote coseimic increase in groundwater levels and discharge rates, respectively. Open circles and squares denote coseimic decrease in the groundwater levels and discharge rates, respectively.

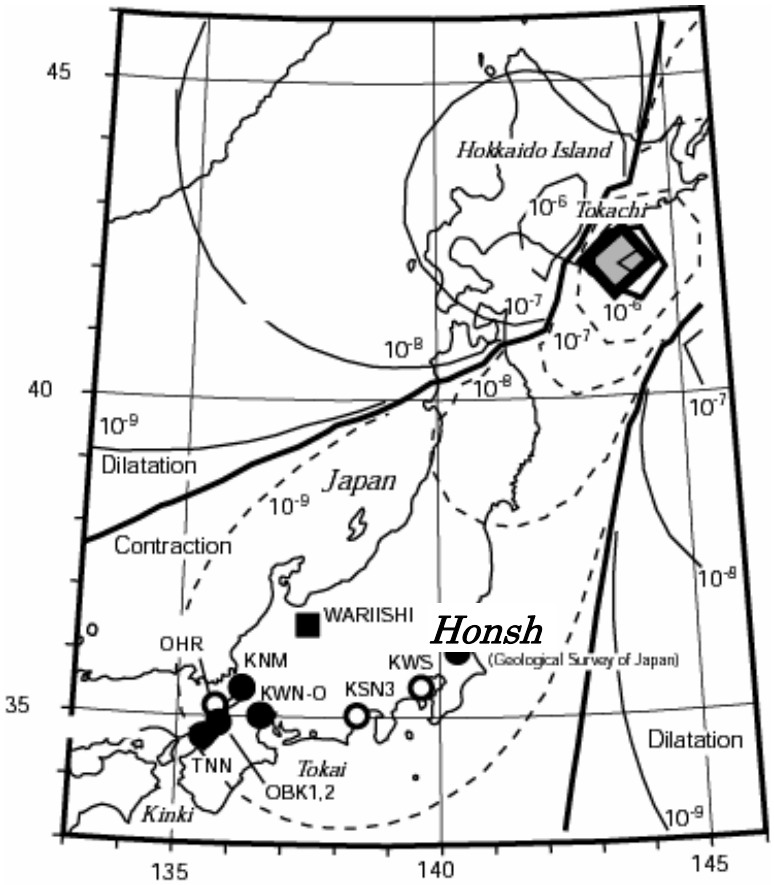

Fig.2

Location of observation wells in Honshu, Japan. A hatched square indicates the fault model (Geographical Survey Institute, 2003). Contours denote the calculated coseismic volumetric strain changes on the surface. The circles and squares have the same meaning as those in Fig.1.

Earthquakes and Mass transport in the crust beneath the Long Valley Caldera - Mammoth Mountain Magmatic Systems

David P. Hill, U.S. Geological Survey, Menlo Park, CA, hill@usgs.gov

Multi-parameter monitoring of the unrest beneath Long Valley caldera and Mammoth Mountain over the past two decades has produced a wealth of clues on the underlying magmatic systems and mass transport within these systems. Key monitoring parameters include seismicity, deformation/geodesy, hydrology, and gas geochemistry. Results from ongoing monitoring efforts augmented by geologic studies, geophysical imaging studies including seismic tomography using both local and teleseismic sources, plus a variety of potential field studies indicate that the current magmatic system in the upper 15 km of the crust beneath the caldera consists of at least two small magma bodies, one of which underlies the resurgent dome. Seismic and gas geochemistry data indicate that the active magmatic system underlying Mammoth Mountain, a 100- to 57-ka dacitic volcano on the southwest rim of the caldera, consists of a plexus of basaltic dikes and sills in the 10- to 25- km depth range. Some (but not all) unrest episodes are clearly associated with upward migration of fluid volumes released from these mid-crustal magma bodies. Although we have made substantial progress in understanding these magmatic systems over the past 25 years, many outstanding questions remain -- including details on their interconnectedness at depth, their lower crustal and upper mantle roots, and the role of tectonic-magmatic interactions in the ongoing magmatic unrest. We expect that data from an instrument package installed last summer at a depth of 2.5 km in the Long Valley Exploratory Well (LVEW) located directly over the inflation center beneath the resurgent dome within the caldera will provide important new constraints on these processes. The LVEW instrument package includes two 3-component seismometers, a borehole dilatometer, a vertical-axis optical strain meter, and a hydrological bypass to track pore variations in pressure in the hole below the instrument package.

Loosening of the interplate coupling in the focal region of the anticipated Tokai earthquake induced by the 2000 seismo-volcanic event in the northern Izu Islands

Akio Kobayashi, Meteorological Research Institute, JMA, akobayas@mri-jma.go.jp

A huge earthquake swarm including five earthquakes with a magnitude of 6 or larger occurred in the summer of 2000 in the sea between Miyake and Kozu Islands, south of the Izu Peninsula, central Japan (Japan Meteorological Agency [JMA], 2000). The continuous GPS observation network of the Geographical Survey Institute (GEONET) revealed that remarkable crustal deformation occurred in a broad area during this event (Kaidzu *et al*., 2000). In order to account for the notable displacement fields around the northern Izu Islands, Nishimura *et al*. (2001) proposed a source model consisting of tensile faults that represent the dyke intrusion, faults of five large earthquakes, and an aseismic shear fault.

Using a similar model, but using GPS data in a broader area from the Kanto to Tokai regions, we obtained optimum source parameters for the displacement fields in each three-month period from May through August, June through September and from July through October. It was shown that although the optimum source models can represent most of the crustal deformation in each three-month period, noticeable eastward or southward displacement residuals were found in Tokai and the surrounding regions in the period from June through September and from July through October, respectively.

In order to account for the displacement residuals, we first examined the residuals to see if they could have originated from a suspension of steady back-slip movement of the Philippine Sea – Honshu plate interface. Deformation residuals during the period of May through August were well-explained by the suspension of back-slip movement in the focal region of the anticipated Tokai earthquake. However, the suspension of back-slip movement was not enough to explain the residuals for the later period event.

To elucidate what has been occurring on the plate interface in the later period, we next performed inversion analyses. The inversion analyses indicated that not only a suspension of back-slip but also a small forward slip in the area beneath Lake Hamana is needed to account for the residual in the period from June to September. In addition, further forward slip in the wide area from Lake Hamana to the northwest is estimated in the later period from July to October, while the back-slip movement resumed under the adjacent focal region of the Tokai earthquake.

The new source models that includes suspension of back-slips and occurrence of forward-slip on the Philippine Sea – Honshu plate interface beneath Lake Hamana in addition to a dyke, earthquakes and a creep-like shear fault located to the west of Miyake Island, explains

very well the evolution of the crustal deformation in Tokai and the surrounding area. Ozawa (2002) pointed out that an aseismic slip on the plate interface in the Tokai area started in October 2000. Although not clearly observed before October due to the deformation caused by the 2000 event, the interplate coupling had already begun to weaken. We consider that the ongoing aseismic slip was a natural consequence of the loosening of the interplate coupling.

We are grateful to the Geographical Survey Institute for providing the GPS data.

References

Japan Meteorological Agency, Recent seismic activity in the Miyakejima and Niijima-Kozushima region, Japan -the largest earthquake swarm ever recorded-, *Earth Planets Space*, 52, i-viii, 2000.

Kaidzu, M., T. Nishimura, M. Murakami, S. Ozawa, T. Sagiya, H. Yarai and T. Imakiire, Crustal deformation associated with crustal activities in the northern Izu-islands area during the summer, 2000, *Earth Planets Space*, 52, ix-xviii, 2000.

Kobayashi, A., T. Yamamoto, H. Takayama and A. Yoshida, Crustal deformation in the Chubu-Kanto region at and after the 2000 seismic and volcanic activity around the northern Izu islands (in Japanese with English abstract), *J. Geodetic Soc. Japan*, 49, 121-133, 2003.

Nishimura, T., S. Ozawa, M. Murakami, T. Sagiya, T. Tada, M. Kaidzu and M. Ukawa, Crustal deformation caused by magma migration in the northern Izu islands, Japan, *Geophys. Res. Lett*., 28, 3745-3748, 2001.

Ozawa, S., M. Murakami, M. Kaidzu, T. Tada, T. Sagiya, H. Hatanaka, H. Yarai and T. Nishimura, Detection and monitoring of ongoing aseismic slip in the Tokai region, central Japan, *Science*, 298, 1009-1012, 2002.

A Study on Seasonal Variation of Leveling Data in the Omaezaki Region

Imakiire Tetsuro, Geographical Survey Institute, Japan, imq@gsi.go.jp

The Geographical Survey Institute (GSI) of Japan has been carrying out leveling surveys in the Omaezaki region, four times per year, since 1981. These leveling surveys revealed that Hamaoka (BM2595) is subsiding about 5mm/yr relative to Kakegawa (BM140-1). Though the rate of subsidence is steady in the long term, we find that seasonal variation overlays the observed trend. The amplitude of seasonal variation is as much as 1cm (peak to peak). Various hypotheses have been proposed for the origin of this variation. As GPS data does not show such significant seasonal variation, it is suspected that the origin of this variation would be a factor which is uniquely related to the leveling observations themselves.

One of the least-likely sources of this variation was atmospheric refraction. However, our study analyzed the statistic parameters of this seasonal variation for 13 sections of the leveling route, and revealed two remarkable features not explainable by atmospheric refraction. If the atmospheric refraction causes the seasonal variation, two characteristics would be expected. 1) The amplitude of variation is proportional to the height difference of two bench marks. 2) The phase of variation is reversed between ascending sections and descending sections. As the compiled data do not show these trends, we suspected that another source of seasonal variation is dominant.

A second suspected source for the seasonal variation is thermal extension of a leveling staff where the invar tape was exposed to the sun. The invar tape of the staff would expand as its temperature increases compared with the tape on the opposite side of the staff. As the effect of the sun varies seasonally, a systematic error may also vary seasonally.

One of the remarkable features of the leveling data in the Omaezaki region which would possibly support this hypothesis is that the seasonal variation seems to have been smaller since 2000. We noted that the difference in seasonal variation is significant after the statistical test on two models.

One possible reason for this phenomenon is the change of the regulations for leveling surveys. GSI defines the standard procedure for surveys. The procedure before July 1999 called for the use of only a tilting level, such as the Wild N3, for leveling purposes. It was also standard procedure that two readings were required for one observation. This procedure was specifically defined for leveling in the Omaezaki region to reduce both the random error for the observations, and the systematic error caused by the level. However, the regulations were changed in October, 1999 as the reliability of automatic levels and digital levels became accepted. Therefore the leveling surveys in the Omaezaki region after October, 1999 were

carried out using automatic or digital levels. Taking only one reading for each observation has been standard procedure since then. The effect of this change to the observation procedure is the shortening of observation time. If the observation time becomes shorter, the time during which the leveling staff is exposed to sunshine also becomes shorter. This could cause the observed seasonal variation of leveling results to become smaller as the effect of the thermal expansion of the invar tape becomes smaller.

Even though we consider more quantitative investigations necessary to confirm this hypothesis, thermal expansion is a possible factor for the seasonal variation of leveling data in the Omaezaki region.

Interpretation of Stress Orientation in the Peninsular Ranges and Coachella Valley Region of Southern California

Robert L. Wesson and William Z. Savage, U.S. Geological Survey, Golden, CO, rwesson@usgs.gov

Details of observations of stress orientation in southern California as inferred from focal mechanism studies have provoked some controversy. Nonetheless, in the region of the Peninsular Ranges, the Coachella Valley, and the Little San Bernardino Mountains where the major faults are parallel, relatively straight for long distances, and the geometry is close to two-dimensional, the interpretations of different workers share certain common characteristics. First, there seems little disagreement that at great distances (>50 km) from the major faults, the principal compression is oriented nearly normal to the strike of the faults. Near the San Jacinto and Elsinore Faults where focal mechanisms are ample both Hardebeck and Hauksson (1999, 2001) and Townend and Zoback (2001, see in particular their Figure 4) agree that the principal compression is oriented at about 40 to 50 degrees to the strike of the faults. Numerous interpretations of the relatively dense geodetic observations in this region are consistent with the notion of steady slip below the seismogenic zone along the Elsinore, San Jacinto, and San Andreas faults at rates consistent with the geologic slip rate data. The observations of stress orientation have been the subject of a lively debate about the strength of the faults in the seismogenic zone. Using 1-D and 3-D dislocation models as well as simple finite element modeling, we show that the principal assumptions required to explain the observations of stress orientation are that slip is occurring on the faults at depth, and that the seismogenic zone is currently locked. In particular, the observations can be explained without reference to the strength of the seismogenic zone except to observe that it is currently locked. The models allow investigation of the effects of the relative magnitudes of the regional stresses and the shear stress perturbations caused by the locked portions of the seismogenic zone on the stress orientations near these major strike slip faults.

Recurrence of earthquake swarms east of the Izu Peninsula, central Japan

Yoshimitsu Okada, National Research Institute for Earth Science and Disaster Prevention, Japan, okada@bosai.go.jp

East of the Izu Peninsula, central Japan, earthquake swarms have been intermittently repeating since June, 1978. Synchronized to the occurrences of the swarms, remarkable crustal deformation has also been repeatedly detected by tiltmeters, strainmeters, leveling surveys, laser distance measurements, and GPS observations. Based on these data, repeated events were successfully modeled as being caused by dyke intrusion. In addition to co-swarm crustal deformation, small precursory crustal deformation signals were found to precede major swarm activities [Okada et al., 2000].

Persistent swarm activity seemed to stop after a major swarm in April, 1998. At the same time long lasting abnormal crustal deformation also seemed to stop. However, after a quiescence of 4 years, minor swarm activity began again in May, 2002 and similar events again started their repetition.

Co-swarm crustal deformations

Due to its high crustal activity, a number of instruments have been installed and frequent surveys were conducted in the eastern Izu Peninsula region. Figure 1 summarizes the results of these observations associated with 30 swarms from the years 1978 – 1998.

From 1978 – 1988, abnormal crustal deformations were mainly detected by repeated surveying and groundwater observations. However, poor time resolution in the survey methods and unstable co-seismic responses in the groundwater observations prevented us from distinguishing whether these abnormal deformations are ongoing or associated with swarms. Co-swarm signals have been detected by a volumetric strainmeter installed at the Higashiizu (HIG) station. These signals were not always believed because they were reported from only one station and their amplitudes were fairly large compared to the epicentral distances. However, a borehole tiltmeter was installed at Ito (KWN) adjacent to the swarm region and recorded a clear co-swarm tilt signal associated with the 8905 event, simultaneously with a strainmeter record at HIG. These were confirmed.

Two months later, a strong swarm, 8907, began and was accompanied by a submarine eruption at Teishi knoll. Data obtained from this event enabled us to establish a dyke intrusion model for the swarm activity in this area [Okada and Yamamoto, 1991]. Successive swarm events and associated crustal deformations could be successfully modeled by the same concept (Figure 2).

Pre-swarm crustal deformations

A careful check of the tilimeter records associated with the repeated swarms led us to discover pre-swarm crustal deformation (Figure 3). Preceding the start of swarm activity, the tiltmeter installed at KWN underwent a gradual tilt movement. The signal has the following characteristics. (1) It is clear only for major swarms. (2) The time before the swarm is several hours to half a day. (3) The signal level is on the order of 0.1 micro-radian. (4) The tilt direction is always NE down and smoothly connects to the initial co-swarm change. From this final characteristic we can consider that the pre-swarm tilt has the same origin as the co-swarm tilt, and we can assume that the cause of the pre-swarm crustal deformation is dyke intrusion at depth.

The phenomena of pre-swarm crustal deformations are also found by another tiltmeter and three-component borehole strainmeter installed adjacent to the KWN station, as well as at the volumetric strainmeter at station HIG.

Recurrence of swarms

After a major swarm in April, 1998, persistent swarm activity seemed to stop. At the same time, long-lasting abnormal crustal deformation also seemed to stop. However, after a quiescence of 4 years, minor swarm activity resumed in May, 2002, and similar events were also repeated during June, 2003 and April, 2004 (Figure 4).

At present we have no definite answers to the following questions. (1) How long will swarm activity continue? (2) Will a major swarm occur in the near future? (3) Will a volcanic event like the dyke intrusion of July, 1989 recur?

References

Okada, Y. and E. Yamamoto, (1991) Dyke intrusion model for the 1989 seismovolcanic activity off Ito, central Japan, J. Geophys. Res., 96, 10361-10376.

Okada, Y., E. Yamamoto, and T. Ohkubo (2000) Coswarm and preswarm crustal deformation in the eastern Izu Peninsula, central Japan, J. Geophys. Res., 105, 681-692.

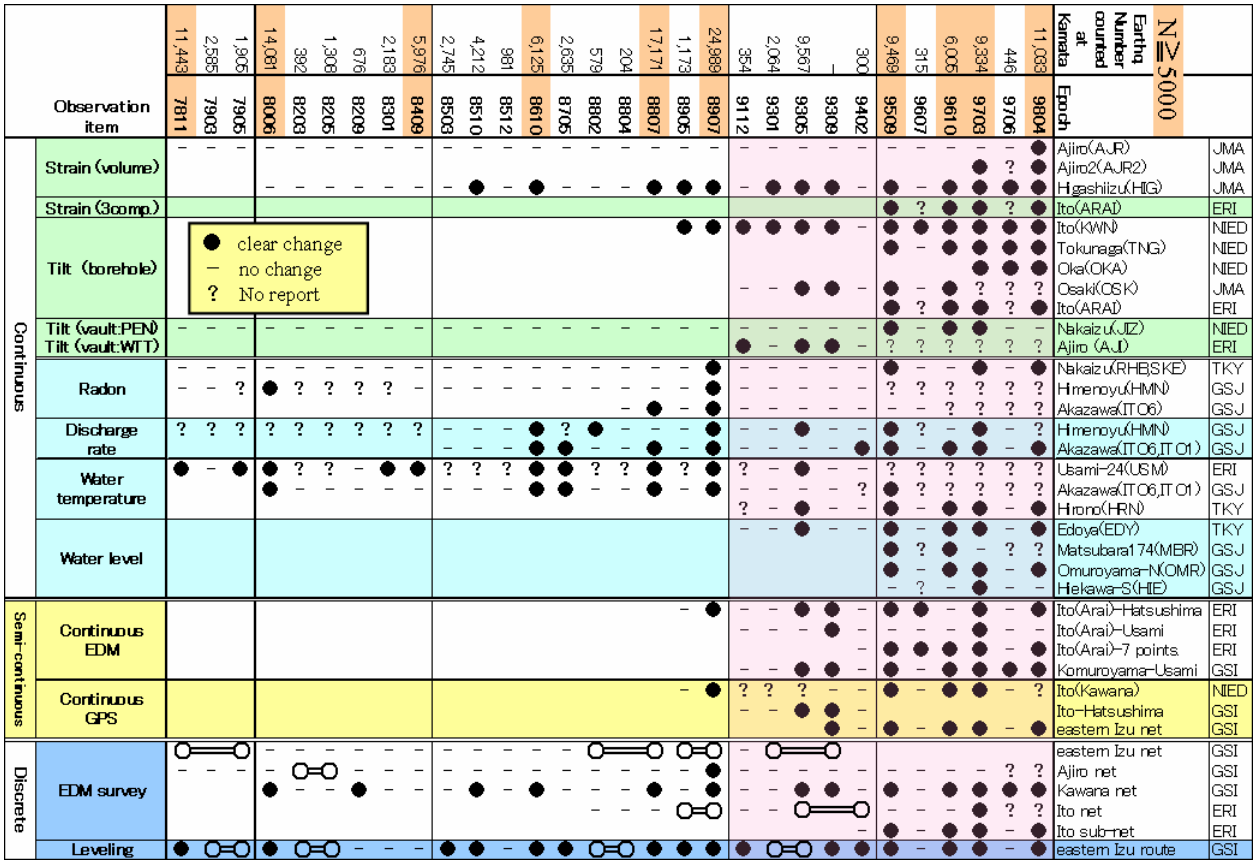

Figure 1. Swarms of the eastern Izu Peninsula and associated strain, tilt and groundwater changes during the past 20 years. (○=○: Effects of several events are contaminated)

Figure 2.

< Top > Tilt down vectors at station KWN associated with a series of swarm events. Tilts are always NE down at the beginning.

< Bottom >

(a) Two vertical tensile fault models, A and B, along the swarm zone. (b) Schematic surface elevation change due to a buried tensile fault whose top and bottom depths are d and D, respectively. (c) Expected tilt-down vectors at station KWN for model A. (d) Expected tilt-down vectors at station KWN for model B.

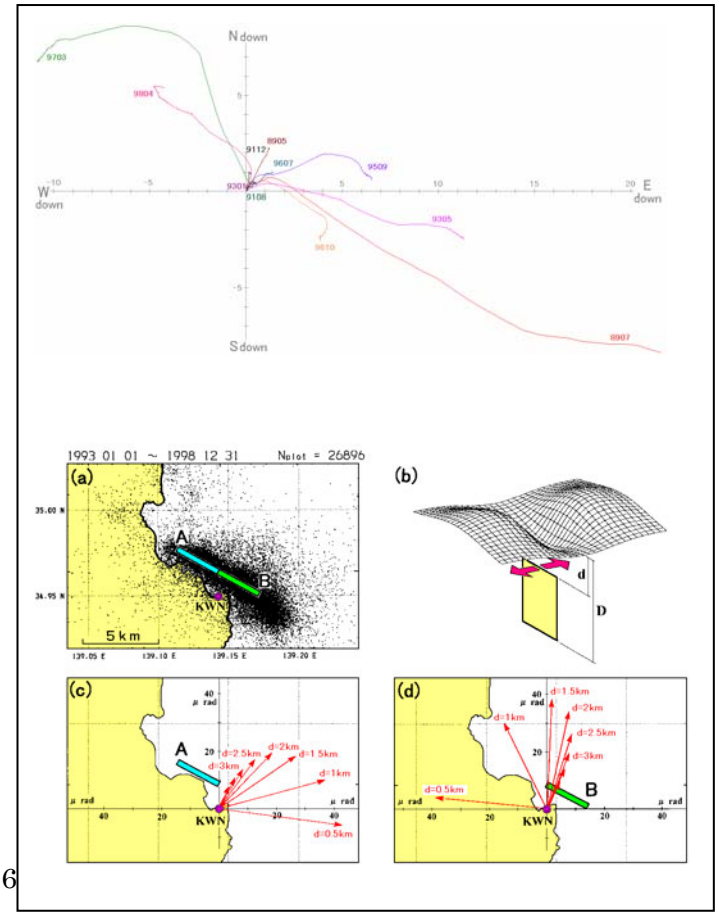

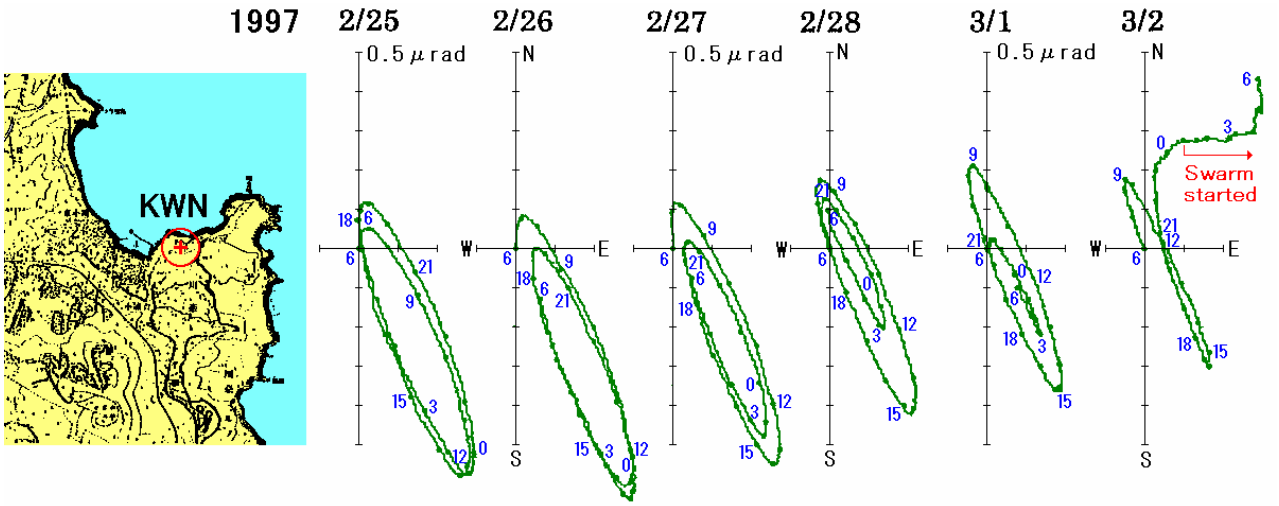

Figure 3. <Top> 24 hours tilt down vectors at station KWN. Numerals show the time points. In the evening of March 2, NE down tilt has begun preceding the swarm onset by several hours.
<Bottom> Tide removed tilt down vectors for each swarm events. Pre-swarm tilting is always NE down.

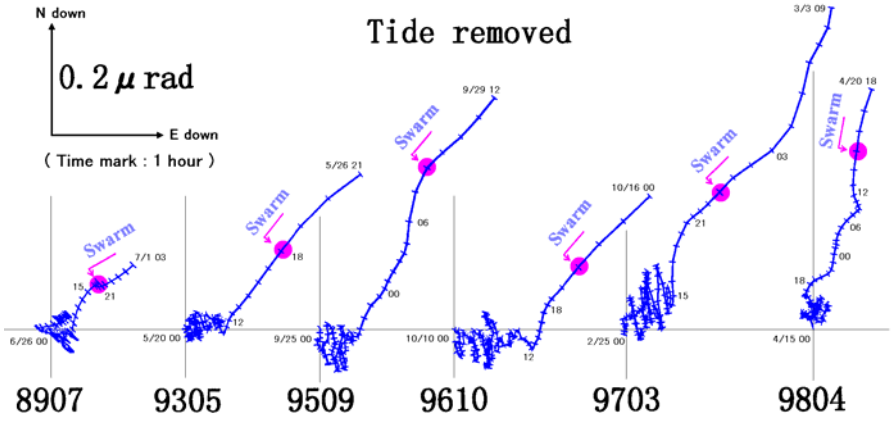

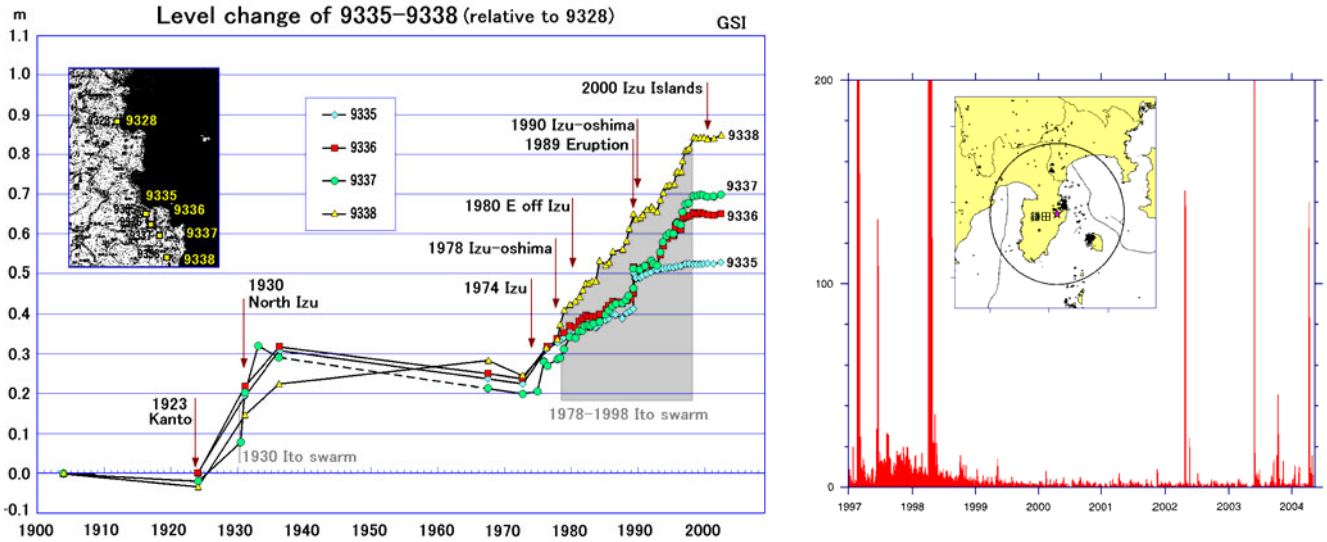

Figure 4. < Left > Crustal uplift at the eastern Izu Peninsula during the recent 100 years (GSI).
< Right > Most recent recurrence of earthquake swarms east of the Izu Peninsula.

Preparing for the San Andreas Fault Observatory at Depth: Results from Site Characterization Studies and the SAFOD Pilot Hole

Stephen Hickman[1], Mark Zoback[2] and William Ellsworth[1]

[1] U.S. Geological Survey, 345 Middlefield Road, Menlo Park, California, hickman@usgs.gov
[2] Dept. of Geophysics, Stanford University, Stanford, California

The San Andreas Fault Observatory at Depth (SAFOD) is a comprehensive project to drill and instrument an inclined borehole across the San Andreas Fault Zone to a depth of 3.2 km as part of the U.S. National Science Foundation's (NSF) EarthScope initiative (www.earthscope.org). SAFOD will answer fundamental questions about the physical and chemical processes controlling faulting and earthquake generation within a major plate-boundary fault. The drill site is located 1.8 km southwest of the surface trace of the San Andreas Fault along a segment of the fault that moves through a combination of aseismic creep and repeating microearthquakes, just north of the rupture zone of the 1966 Parkfield M=6 earthquake. SAFOD will permit direct measurements of the physical conditions (stress, fluid pressure, permeability, temperature, etc.) within the fault zone; recovery of fault rocks and fluids for laboratory analysis of fluid-rock interaction, physical properties and deformational behavior; and emplacement of instruments within the near-field environment of repeating (M~2) earthquakes to monitor the evolution of physical conditions within the fault zone during multiple earthquake cycles.

A wide variety of geological and geophysical site characterization investigations have been carried out since the SAFOD project was first proposed about 12 years ago. These studies include deep electromagnetic soundings, gravity and magnetic profiles, high-resolution seismic reflection and refraction profiles, thermal and geochemical studies in shallow wells, geologic mapping, and deployment of a 70-station seismic network: – the Parkfield Area Seismic Observatory – to facilitate microearthquake relocations and development of a 3-D velocity model. In the summer of 2002, a 2.2-km-deep, vertical pilot hole was drilled at the SAFOD site as a collaborative effort between the International Continental Drilling Program, NSF and the U.S. Geological Survey. A 32-level, 3-component, high-frequency seismic array was installed in the pilot hole at the conclusion of drilling for observation of local microearthquakes and downhole recording of controlled-source seismic experiments conducted in 2002 and 2003.

As a result of the comprehensive suite of investigations surrounding the SAFOD site, it has been possible to better define the overall structure and geophysical setting of the San Andreas Fault Zone at Parkfield and to improve the location accuracy for the repeating microearthquakes being targeted by SAFOD. As a result, the accuracy with which we are able to

locate the 100 m ‘‘patches’’ of the fault producing the repeating earthquakes we are attempting to intersect with SAFOD is now about 100-200 m. Analysis of the extensive suite of open-hole logs and cuttings from the pilot hole has helped characterize the in-situ state of stress, heat flow, physical properties, alteration mineralogy and uplift history in the granitic basement adjacent to the San Andreas Fault. These investigations also provided critical information on the locations of secondary fault zones and velocity discontinuities that were used to design the current SAFOD scientific and operational plan. This geophysical and geological model is now being tested and refined as we drill toward the San Andreas Fault with SAFOD.

SAFOD 2004 – Overview of Scientific Results from Phase 1 and a Look-Ahead to Phases 2 and 3.

Mark D. Zoback[1], Stephen H. Hickman[2], William L. Ellsworth[2]
[1]Department of Geophysics, Stanford University, Stanford, CA, zoback@stanford.edu
[2]U.S. Geological Survey, Menlo Park, CA

On September 16, 2004, SAFOD reached the planned total depth for Phase 1. After drilling vertically to a depth of ~ 1.5 km at a site 1.8 km from the San Andreas Fault, the SAFOD drillhole is now deviated 54 degrees from vertical and has drilled 1.1 km toward the San Andreas fault, aiming directly at a patch of fault producing repeating M~2 microearthquakes at 3 km depth. The current vertical depth of the hole is 2.5 km. During drilling, gas emanations (He, CO_2, CH_4, H_2, Rn, etc.) were continuously monitored, cuttings from the well were sampled at 3 m intervals, cores have been obtained from two depths and comprehensive geophysical measurements have been carried out in the hole.

The successful 2.2-km-deep, vertical SAFOD pilot hole was drilled into fractured granite at the same drillsite. Geophysical models suggested we would continue to drill through fractured granite until we encountered the highly deformed fault rocks of the San Andreas Fault Zone. However, when the main hole was only 213 m northeast of the pilot hole, sedimentary rock was encountered after drilling through a fault and the remainder of the hole was drilled in sandstone, with intervals of claystone and shale. As this abstract is being written, a suite of geophysical logs is being obtained to characterize the physical properties of the rocks already penetrated, the degree of faulting in these rocks and the *in situ* stress state. Three sets of data are being obtained in the SAFOD borehole to help reduce uncertainties in the exact location of the target microearthquakes: P- and S- velocity logs are being obtained, an 80-level seismic array will be deployed in November to record surface shots to better constrain existing seismic velocity models, and monitoring of microearthquakes in and near the target zone will go on utilizing a seismometer at the bottom of the main hole until Phase 2 drilling begins in early summer of 2005.

One of the highlights of the downhole measurements program was a mini-frac test at ~1.5 km. The magnitude of the least principal stress obtained in this test confirms the strike slip/reverse stress state derived in the pilot hole (where no mini-fracs could be done) and helps establish the stress field outside the active fault zone. A fluid sampling test will be carried out during the hiatus in drilling between Phases 1 and 2 to obtain uncontaminated fluid samples and another mini-frac stress measurement will be obtained at that time, at greater depth and much closer to the San Andreas Fault.

Numerous monitoring activities are underway related to construction of the SAFOD observatory. An integrated seismic, strain and pore pressure instrumentation sonde is being developed for deployment in the pilot hole next spring. In addition, a fiber optic laser strainmeter will be deployed behind casing in the main SAFOD hole at the end of September. The 80-level, high temperature seismic array mentioned above is being evaluated as a possible instrumentation backbone used for the permanent deployment of seismic (and other) sensors in the main hole when coring operations come to an end in 2007.

Stress changes and non-linear scaling of slip on faults with fractal roughness: Implications for modeling of fault systems

James H. Dieterich, U.S. Geological Survey, Menlo Park, CA, jdieterich@usgs.gov

A long-established representation of faults in standard earthquake models is that of a single planar slip surface embedded in an elastic medium. The planar fault representation is, of course, highly idealized. Fault surfaces have irregularities over a very wide range of wavelengths and form branching structures and networks. Slip on geometrically complex faults involves processes that do not exist for planar faults. Geometric features inhibit slip and produce slip interactions through changes of shear and normal stress at all scales. This study employs numerical models of single faults with random fractal roughness that undergo slip under quasi-static conditions. Though simpler than fault systems in nature, the models incorporate this added category of sliding processes, which exemplifies geometrically complex faults. Characteristics of slip on the fractal faults, which are not evident in planar fault models or multi-segment models with a narrow range of interaction scales, include geometrically-controlled fluctuations of slip along the fault, and a systematic decrease of total slip with increasing amplitude of fault roughness. Also, the amplitude of fault roughness affects the overall shape of the slip distribution along the fault. Several aspects of model behavior are sensitive to system size. For example, as the number of fault elements in the model increases, the relationship between slip and fault length becomes strongly nonlinear. This breakdown of linear scaling, which is characteristic of flat faults, may have implications for scaling of earthquake source parameters. This scale effect also indicates that large scale models of regional earthquake processes and fault systems, may in certain circumstances, give results that depend strongly on model size (i.e. the number of elements used to resolve small scale features). A feature of geometrically complex faulting is that large local stresses develop in response to the complexity. In nature these stresses cannot increase without limit – this suggests that local yielding or faulting must be an integral part of the sliding process and will probably have to be considered in large scale modeling efforts.

Experimental and Geological Studies on Slip Process in the Deep Extensions of Seismogenic Faults

Koji Masuda, Miki Takahashi, Keigo Kitamura, Takashi Arai[1],
Koichiro Fujimoto[2], and Norio Shigematsu[3]

Institute of Geology and Geoinformation, Geological Survey of Japan,
National Institute of Advanced Industrial Science and Technology (AIST),
AIST Tsukuba Central 7, Tsukuba, 305-8567, Japan, koji.masuda@aist.go.jp
1 Present address: National Institute of Technology and Evaluation (NITE), Tokyo, Japan
2 Present address: Tokyo Gakugei University, Koganei-city, Tokyo, Japan
3 Present address: Chiba University, Chiba, Japan

Understanding physical and chemical processes in the deep extent of seismogenic fault zones is very important, since the main rupture of most large intraplate earthquakes initiates at the base of the seismogenic zone. Geological studies on exhumed fault zones, geophysical measurements of natural fault materials from seismogenic zones, and laboratory experimental studies under high-pressure and high-temperature conditions are carried out at the Geological Survey of Japan, AIST.

Large inland earthquakes can occur directly below populated areas causing enormous damage and loss of human life. Although it is essential to understand the mechanisms by which intraplate earthquakes occur, and to establish physics-based forecast methods, the mechanism by which inland earthquakes occur is currently poorly understood compared to interplate events.

In order to understand the earthquake generation process, we need to understand the frictional and rheological properties of fault zone materials under high-pressure and high-temperature conditions. Laboratory data on the frictional properties of fault surfaces of fault zone rocks are useful for understanding the slip process in deep extents of seismogenic zones. We designed and constructed an original Japanese-type gas-medium deformation apparatus. The frictional properties of mylonite, feldspar, and quartz under high-pressure and high-temperature conditions were obtained. In the laboratory study, we used information on the natural fault materials based on the results of the geological study. We conducted geological studies on an exhumed seismogenic fault zone in Japan, the Hatagawa Fault Zone, to characterize fault zone materials and fault zone structure. The physical properties of such materials and country rocks (seismic velocities, electrical resistivity, permeability) were also measured in the lab under the expected *in situ* conditions.

We carried out a series of conventional triaxial compression tests of mylonite at a

constant displacement rate. We then analyzed the stress-strain relation and the frictional behavior of the fault surface formed in the tests. Mylonite samples were taken from an exposed brittle-ductile transition zone, the Hatagawa Fault Zone, northeast Japan, and tested under hydrothermal conditions. Even under the same effective confining pressure, the presence of pore water dramatically reduces the peak shear stress at a temperature regime higher than 600C. The frictional properties of fault surfaces formed during the deformation tests were investigated. In the dry conditions, stick-slip behaviors were observed at room temperature and at 200C. For the temperature range up to 600C, frictional forces were almost identical. In wet conditions, we did not observe stick-slip behaviors at all temperature ranges. The frictional force decreased as the temperature increased. Fluids such as water in the deep crust may play an important role in the deformation process.

We conducted frictional experiments by using feldspar and quartz gouges (about 3 micron diameter) under high-pressure and high-temperature in both wet and dry conditions. These experiments were conducted by the velocity-stepping test. Temperatures varied from room temperature to 600C. In dry conditions, experiments were conducted under a confining pressure of 150MPa. In wet conditions, pore water pressure was applied up to 50MPa under a confining pressure of 200MPa. Samples were put between upper and lower sawcut aluminum cylinders. The values for a-b of quartz and feldspar were positive under the dry conditions from room temperature to 600C. On the other hand, velocity weakening of quartz gouge is seen at around 300C, and the negative region occurs from 200C to 400C. Velocity weakening of the feldspar gouge was observed from 150C to 450C, and was more apparent than that of the quartz gouge. If true, feldspar would play a more important role than quartz in the velocity weakening region observed with the granite gouge. These frictional properties are discussed with the texture of samples by the SEM observations.

Measuring Fault Slip - Why and How?

Ken Hudnut, U.S. Geological Survey, Pasadena, CA, hudnut@usgs.gov

To improve our understanding of earthquake physics, we must make observations of parameters that determine friction on the fault surface during rupture. Observables may include, for example, 3D point trajectories to fully record near-field dynamic phenomena such as slip pulses, as well as details of slip variation along strike. We have devised and tested new methods for observing these quantities in nature. First, we observed the details of topography along the 1999 Hector Mine surface rupture using Airborne Laser Swath Mapping. This allowed us to estimate slip variation along-strike of the fault, in some places, with higher spatial resolution than has ever before been possible. The results are, however, complex due to ground surface irregularity and pre-existing topographic features. Evidently, slip variations along strike are greater than previously recognized, implying extreme slip heterogeneity. We provide a simple explanation for how such rapid slip variations could provide the source for high-frequency seismically radiated energy, at least in the near field. Second, we have developed the concept for, and built a working prototype of, a GPS Fault Slip Sensor spanning the San Andreas fault. In addition to augmenting seismic early warning systems, such instrumentation could also provide unique records of near-field ground motions. Inertial sensors such as seismic instruments are not able to differ between a tilt and an acceleration, whereas GPS measurements can differentiate these, and can be made with respect to an absolute frame of reference. Other practical limitations exist, however, in both kinds of instrumentation and we will describe how they may best be integrated into a system that will achieve both the scientific observational objectives and support earthquake early warning.

Earthquake Forecast Testing

David D. Jackson, Yan Kagan, Agnes Helmstetter, UCLA, djackson@ucla.edu
Danijel Schorlemmer, and Stefan Wiemer, ETH Zurich
Matt Gerstenberger, IGNS New Zealand

We define an earthquake forecast as a statement of probability density in location, magnitude, time, and focal mechanism variables. Most such forecasts can be tested using a simple likelihood ratio method. We illustrate one method to be applied to the Regional Earthquake Likelihood Models (RELM) project of the Southern California Earthquake Center (SCEC). Several forecast models are being developed and others are welcome. Various models include fault geometry and slip rates, seismicity, strain, and stress interactions. With some adaptation, each can be expressed as a vector of earthquake occurrence rates defined over bins of latitude, longitude, depth, magnitude, time, strike, dip, and rake. We would test models pair-wise, requiring that both use the same bins. We offer a standard "menu" to encourage standardization. One menu item includes five-year forecasts of magnitude 5.0 and up on a 0.05 degree grid. The five-year forecast may be appropriate for testing hypotheses of stress shadows from large earthquakes. Interim progress will be evaluated yearly, but final conclusions would be based on cumulative five-year performance. The second category includes short-term forecasts of quakes above magnitude 4.0 on a 0.05 degree grid, evaluated and renewed daily. Competing pairs of forecasts with different magnitude, space, and time sampling are welcome.

Foreshocks, main shocks, and aftershocks will be counted as equivalent and considered as point sources at the hypocenter. For each forecast pair we compute alpha, the probability that the first would be wrongly rejected in favor of the second, and beta, the reverse. To compute alpha and beta we need the distribution of likelihood scores under each hypothesis, estimated by simulations. No hypothesis will be the a-priori favorite. Results will be archived on the RELM web site.

What controls slip heterogeneity- prestress, fracture energy, or sliding friction?

Brad Aagaard, U.S. Geological Survey, Menlo Park, CA, baagaard@usgs.gov
and Thomas Heaton, California Institute of Technology

We are exploring the physics of earthquake ruptures to understand what controls slip and stress heterogeneity. We consider many variations in the fault friction model and seek a set of parameters that allows the system to evolve into a stable heterogeneous state. In other words, earthquake ruptures with heterogeneous slip are able to occur across a wide range of length scales. We test friction models with and without shear restrengthening (friction rises as slip rate drops) and with and without spatial variations in the fracture energy and dynamic sliding stress.

Results from 3-D finite-element dynamic rupture simulations of earthquakes with magnitudes between 5.0 and 7.7 on a planar strike-slip fault show that:

(1) heterogeneous prestress with no shear restrengthening, uniform fracture energy and uniform dynamic sliding stresses rapidly evolves into a nearly homogeneous stress state with earthquakes that only rupture the entire fault and produce distributions of slip that are much too smooth;

(2) heterogeneous prestress with shear restrengthening, uniform fracture energy and uniform dynamic sliding stresses slowly evolves into a homogeneous stress state with earthquakes that rupture larger and larger portions of the fault and produce distributions of slip that are too smooth;

(3) heterogeneous prestress with no shear restrengthening, heterogeneous fracture energy and heterogeneous dynamic sliding stresses evolves into a slightly heterogeneous stress state with too many large earthquakes that produce reasonable distributions of slip;

(4) heterogeneous prestress with shear restrengthening, heterogeneous fracture energy and heterogeneous dynamic sliding stresses evolves into a heterogeneous stress state with a wide variety of earthquake sizes that produce realistic distributions of slip.

As the stress state on the planar fault tends toward a more homogeneous distribution, the slip distributions become smoother and fail to exhibit the degree of heterogeneity seen in kinematic source inversions. The set of parameters that appear to produce the most realistic

conditions (set 4) yields faults that are in a critical state and can fail across a wide range of length scales with slip distributions that have more appropriate levels of heterogeneity. This set of parameters might also be a proxy for nonplanar fault geometry; we suspect that nonplanar geometry coupled with relatively homogeneous friction parameters would yield similarly realistic behavior.

GPS Data Products for Solid Earth Science

Frank Webb, Sharon Kedar, Danan Dong, Sue Owen, Don Argus, and Brian Newport, Jet Propulsion Laboratory, Pasadena, CA, fhw@jpl.nasa.gov

Yehuda Bock, Ruey-Juin Chang, Peng Fang, Jeff Genrich, Paul Jamason, Linette Prawirodirdjo, David Malveaux, and Michael Scharber, Scripps Institute of Oceanography, La Jolla, CA

Nancy King, and Keith Stark, U.S. Geological Survey, Pasadena, CA

Over the past decade, regional and global networks of continuously operating GPS ground stations have been deployed to monitor Solid Earth deformation, and to support NASA Earth Science Enterprise (ESE) priorities and flight projects. At the forefront, and the focus of this project, is the 250-station Southern California Integrated GPS Network (SCIGN), a multi-agency effort jointly sponsored by NASA, NSF, USGS, and the W.M. Keck Foundation, under the umbrella of the Southern California Earthquake Center (SCEC). Over the next five years, SCIGN will become an integral part of the multi-agency, multi-disciplinary Plate Boundary Observatory (PBO), an observatory of high-precision geodetic instruments spanning western North America. This project is intended to be a NASA contribution to PBO and the larger NSF-led EarthScope initiative while concurrently meeting objectives of NASA's ESE.

Our project was selected under the NASA REASoN CAN in 2003 to enhance the delivery of GPS data and metadata products using modern IT methodology, and to produce and disseminate an entirely new set of higher-level data products to a larger community, including scientists, government agencies (Federal, State, and Local), surveyors, and GIS professionals building on current capabilities within SCIGN for data archiving, information systems, and data analysis. While the project focus is on producing data and products from SCIGN, the tools developed will be designed to be extensible to other and larger GPS and other networks of geophysical instruments.

An attempt to image earthquake fault planes and asperities by DD tomography for three large shallow inland earthquakes in Japan

Akira Hasegawa and Tomomi Okada, Research Center for Prediction of Earthquakes and Volcanic Eruptions , Tohoku University, Japan, rikako@aob.geophys.tohoku.ac.jp

It has gradually become clear that the asperity model is applicable to interplate earthquakes in the NE Japan subduction zone. Although we have to continue examining the applicability of the asperity model to earthquake occurrence, it is important to investigate the cause of asperity formation. Looking into the earthquake fault zone in detail is indispensable for this purpose.

We applied the double-difference tomography method (Zhang and Thurber, 2003) to aftershock data of three large, shallow earthquakes that occurred recently to compare the slip distribution of the mainshock rupture with seismic velocity distribution along the fault plane (Okada et al., 2004a, b, c). The results show that the fault plane was imaged as a low velocity zone for the M7.3 1995 Southern Hyogo (Kobe) earthquake, and as a zone of steep velocity change for the M6.4 2003 Northern Miyagi earthquake, but any systematic structure corresponding to the fault plane was not imaged for the M7.3 2000 Western Tottori earthquake. For the three events, large slip areas of the mainshock rupture (asperities) are distributed in high velocity areas on the fault plane, avoiding low velocity areas. The present observations provide important information on the cause of the formation of asperities, and strongly suggest the possibility of imaging asperities of large earthquakes before their occurrences.

The Community Modeling Environment of the Southern California Earthquake Center: An Information Infrastructure for Earthquake Science

Thomas Jordan, Southern California Earthquake Center, University of Southern California, Los Angeles, CA, tjordan@usc.edu

The Southern California Earthquake Center (SCEC), under sponsorship from NSF and the USGS, has taken a system-level approach to two major problems of earthquake science: (1) the *dynamics of fault rupture*—what happens on a time scale of seconds to minutes when a single fault breaks during a given earthquake—and (2) the *dynamics of fault systems*—what happens within a network of many faults on a time scale of years to centuries to produce the sequencing of earthquakes in a given region. These problems are highly nonlinear and coupled to one another through the complex processes of brittle and ductile deformation of the lithosphere. Fully three-dimensional (3D) simulations of fault-rupture and fault-system dynamics are challenging computational problems, but they are now becoming possible through the increasing availability of terascale computing resources. SCEC has embarked on an ambitious program to integrate physics-based models into a new scientific framework for seismic hazard analysis (SHA) and risk management. This framework has been formulated in terms of four basic "computational pathways." Pathway 1 is an SHA computational framework that supports a variety of earthquake forecast models and intensity-measure relationships, primarily through the OpenSHA software (Field et al., 2004). Pathway 2 utilizes the predictive power of wavefield simulation in the construction of intensity-measure relationships. Pathway 3 incorporates fault-system and rupture-dynamics models into earthquake forecasts. Pathway 4 assimilates various types of data into the structural representation of Southern California required by the other pathways. This presentation will summarize SCEC's progress in developing a Community Modeling Environment (CME) that maintains the cyberinfrastructure for the development of these computational pathways and the automation of their configuration and execution. Through several examples, I will show how the SCEC/CME can function as a collaboratory for knowledge quantification and synthesis, hypothesis formulation and testing, data conciliation and assimilation, and prediction.